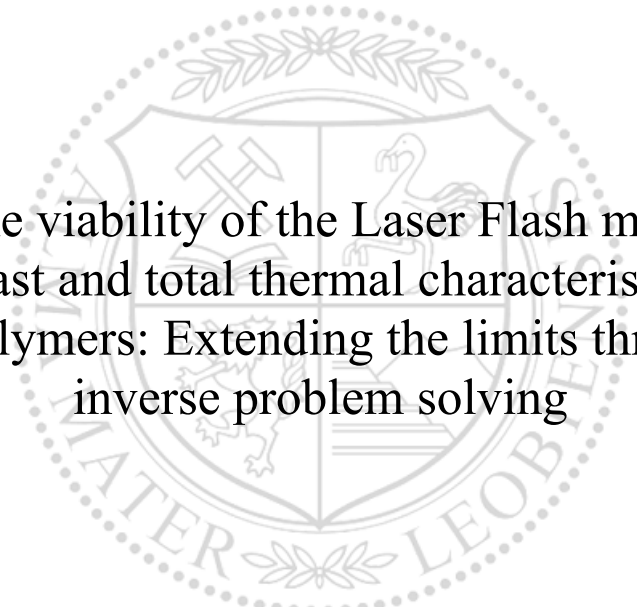Chair of Materials Science and Testing of Polymers

Master's Thesis

On the viability of the Laser Flash method
for fast and total thermal characterisation
of polymers: Extending the limits through
inverse problem solving

David Rapp, BSc

September 2021

MONTANUNIVERSITÄT LEOBEN
www.unileoben.ac.at

EIDESSTATTLICHE ERKLÄRUNG

Ich erkläre an Eides statt, dass ich diese Arbeit selbständig verfasst, andere als die angegebenen Quellen und Hilfsmittel nicht benutzt, und mich auch sonst keiner unerlaubten Hilfsmittel bedient habe.

Ich erkläre, dass ich die Richtlinien des Senats der Montanuniversität Leoben zu "Gute wissenschaftliche Praxis" gelesen, verstanden und befolgt habe.

Weiters erkläre ich, dass die elektronische und gedruckte Version der eingereichten wissenschaftlichen Abschlussarbeit formal und inhaltlich identisch sind.

Datum 12.09.2021

Unterschrift Verfasser/in
David Rapp

PCCL

Polymer Competence Center Leoben

David Rapp BSc: *Master thesis,* On the viability of the Laser Flash method for fast and total thermal characterisation of polymers: Extending the limits through inverse problem solving
© August 2021

SUPERVISORS:
Univ.-Prof. Dipl.-Ing. Dr. mont. Gerald Pinter
Dipl.-Ing. Dr. mont. Mario Stephan Gschwandl

LOCATION:
Leoben

TIME FRAME:
February 2021 - August 2021

I dedicate this to Alexandra.

"Wir müssen wissen.
Wir werden wissen."

David Hilbert

ABSTRACT

The determination of thermophysical material properties is an important aspect for modern day technology. This can be attributed to the rapid advance of numerical simulations throughout the industries and the generally rising academic interest in thermodynamics, as a branch of physics, itself. Many common legacy testing approaches for the acquisition of such properties are slow, or not used to their fullest potential - either by relying on steady-state techniques, or lacklustre instrumentation. Only obtaining the bare minimum of data seems wasteful as high-performance computing becomes broadly available; and data-driven models, machine learning and artificial intelligence systems achieve new breakthroughs by the day. This thesis focuses on the laser flash method (or "Laser Flash Analysis" – LFA), which is used to determine the thermal diffusivity of a substance. The aim is to point out how this method could readily be improved, to also provide thermal conductivity and volumetric heat capacity of a substance, which potentially could eliminate the need for other measurements and thus save time and cost. This is achieved by two different approaches: improving the instrumentation and inverse problem solving. We propose a novel model for the inverse problem and provide other conceptions, which could contribute to the solution by other means, i.e. through statistical thermodynamics. Experimental proof is given by applying these concepts on six different thermoplastic materials and comparing the results against otherwise measured properties. We also consider possible culprits of this method, specifically for polymers. We found evidence, that one of the most important influence on this measurement method are the optical properties of polymers, therefore the modification of them (i.e. by graphite coating) has to be subjected to further research. Because the accuracy and the precision of our crudely simplified model still require further improvements, we discuss possible reasons and are able to provide guidance for future adoptions.

Key words: inverse engineering / laser flash method / LFA / polymer thermodynamics / polymer testing / thermal diffusivity / thermal conductivity / specific heat capacity

KURZFASSUNG

Die Bestimmung von thermophysikalischen Materialeigenschaften ist ein wichtiger Aspekt in der modernen Technik. Dies kann auf die steigende Popularität von numerischen Simulationen in allen Industrien, und auf das allgemein steigende akademische Interesse an der Thermodynamik an sich - als Teilgebiet der Physik – zurückgeführt werden. Viele herkömmliche Prüfverfahren zur Erfassung dieser Eigenschaften sind langsam, kaum automatisierbar, oder schöpfen ihr mögliches Potential nicht voll aus - entweder, weil sie sich auf stationäre (zeitunabhängige) Verfahren stützen, oder unzureichend instrumentiert sind. Unter dem Aspekt der steigenden Verfügbarkeit von Hochleistungsrechnern, dem Vormarsch von datengestützten Modellen, maschinellem Lernen und künstlicher Intelligenz, erscheint es verschwenderisch, Daten nicht möglichst umfassend zu akquirieren und auszuwerten. Im Mittelpunkt dieser Arbeit steht die Laser-Flash-Methode (oder "Laser Flash Analysis" - LFA), die zur Bestimmung der Temperaturleitfähigkeit verwendet wird. Es soll aufgezeigt werden, wie einfach diese Methode verbessert werden kann, um auch die Wärmeleitfähigkeit und die volumetrische Wärmekapazität eines Stoffes zu bestimmen. Dadurch könnten möglicherweise andere Messungen überflüssig werden und somit Zeit und Kosten gespart werden. Das wird durch zwei verschiedene Ansätze erreicht: Verbesserung der Instrumentierung und inverse Problemlösung. In dieser Arbeit wird ein neuartiges Modell zur Lösung der beschriebenen inversen Problemstellung entwickelt und präsentiert. Weiters werden Konzepte vorgestellt, die über andere Ansätze zur Lösung führen könnten, wie z.B. statistische Thermodynamik. Der experimentelle Beweis wird durch die Anwendung dieser Konzepte auf sechs verschiedene thermoplastische Materialien, und den Vergleich der Ergebnisse mit anderweitig gemessenen Eigenschaften erbracht. Wir betrachten darüber hinaus mögliche Schwachstellen dieser Messmethode, speziell für Polymere. Es konnten Hinweise gefunden werden, dass einer der wichtigsten Einflüsse auf das Prüfverfahren die optischen Eigenschaften der Polymere sind, weshalb deren Modifizierung (z.B. durch Graphitbeschichtung) einer genaueren Betrachtung unterzogen werden muss. Da die Genauigkeit und Präzision unseres grob vereinfachten Modells noch Verbeserungen zulässt, diskutieren wir mögliche Gründe und können Verbesserungsvorschläge für zukünftige Adaptierungen geben.

ACKNOWLEDGEMENTS

A PERSONAL ACKNOWLEDGMENT:

Much of the motivation that benefited the successful progression of this thesis was drawn from the goodwill and support of Mario, who gave me the freedom to work on my own ideas, whilst still committing to this thesis with fruitful discussions and goal-driven mentoring. Thank you for everything. Furthermore, I'd like to thank Prof. Pinter, without his academic supervision this thesis would have not been possible. I'm grateful for all supportive colleagues at the PCCL Leoben, and pledge to return each favour and act of kindness I received. The exponentially rising efficiency curve of my work, especially towards the finish-line, would have never been possible without my loving girlfriend Alexandra. Much of what I've achieved throughout the last years, is owed to her. Last but not least, I need to acknowledge my parents, who respected each and every major decision in my life and enabled me to study.

CONTENTS

MOTIVATION AND AIM

1.1 THE IMPORTANCE OF MATERIAL DATA

The relevancy of research in the field of material testing is best explained by the usage of thereby generated data. Whether it is a mechanical engineer designing new components for machinery or consumer products, a material scientist evaluating the properties of newly composed polymer formulations or metal alloys, or a process technician striving to maximize productivity and yield; all of them rely on quantifiable material data to compare, calculate and conclude. Arguably any work in the field of material science stands and falls with thoroughly designed experiments, that enable diligent and comprehensible reduction of generated data for convenient every-day usage. A sector in which precise material properties are particularly important is the simulation and modelling industry. To accurately transfer reality onto a numerical model, either a simplified and scalable model has to be fitted to an expected outcome, or a more complex and physically accurate model needs to incorporate precise parameters and well-defined boundary conditions. Figure 1 shows market data (increasing revenues and forecasts) of the simulation and modelling industry worldwide [76] – revealing that this segment is a growing multi-billion-dollar industry. This clearly illustrates increasing adoption of numerical problem-solving approaches, such as the Finite Element Analysis (FEA) throughout different industries worldwide.

There are a variety of reasons for this trend to exist, i.e. for any arbitrary component development cycle, some of the most notable benefits might be considered as:

1. Arranging the effort so that a greater proportion is scheduled within in an earlier stage of the process, cost inefficient corrections at later stages can be omitted (front-loading); time-to-market may be shortened [80].

2. Proof of concepts are feasible, regardless of the projected complexity. Thereby, the economic risk of failure during development can be significantly reduced and unconventional approaches may not be automatically disregarded.

3. Interfacing novel machine learning (ML) algorithms / artificial intelligence (AI) systems with an optimization problem makes it possible to link the initial task to a numerical model that can be solved automatically [40].
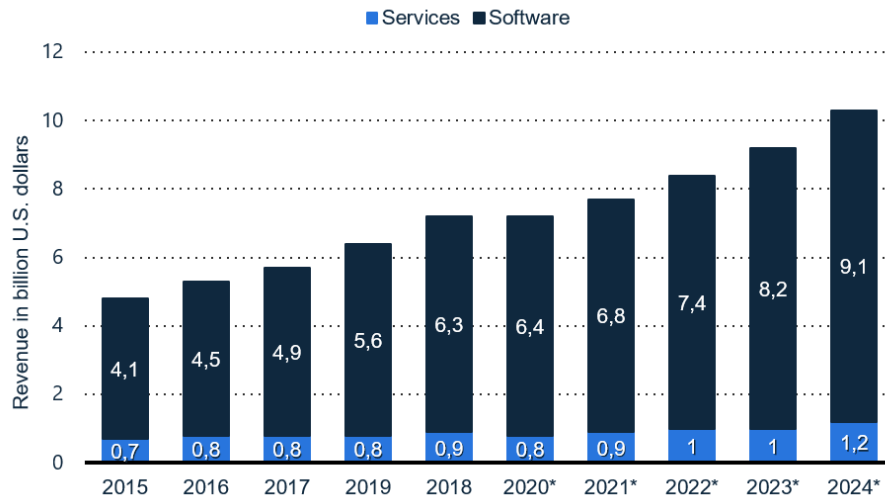
Figure 1: Growing revenues and forecasts for the simulation and modeling industry [76]

Despite the frequent misuse of AI as a buzzword, real benefits and increasing successful adoption can be seen throughout industrial branches. Noteworthy recent use-cases reach from the Google team that managed to deploy an algorithmic machine learning method for fast microchip design [63]; to the company DeepMind (coincidentally also acquired by Google), which achieved breakthrough progression in the prediction of protein folding [13] – potentially boosting future vaccine and drug development. Notably, the microstructure, and thus the properties of polymers, may also be derived through chain folding considerations [43]. On these grounds, there is no reason to discard the idea, that similar ML/AI approaches would not also yield fruitful insights and open ways for novel macromolecular design attempts.

As mentioned above, with rising adoption of FEA within designing and production processes, the overall importance of reliable material data increases, and therefore the significance of material testing. Traditional approaches for designing components typically rely on standardized methods to acquire properties, and often use semiempirically derived formulations to calculate whether the design is of sufficient strength, stiffness, etc. for its use-case. As the standardization implies, material properties are often merely agreed upon metrics, with more or less precise physical meaning. While the traditional procedure certainly holds its ground due to experienced professionals and easy deployment for quick estimates, a lot of generated data seems to be lost in this process, or not even recorded – as a consequence of scarce instrumentation.

A good example of an already used process that provides a strong case for the benefits of leveraging the interconnection between material testing and simulation, is the software package LS-OPT® (DYNAmore GmbH Stuttgart, Germany). In essence, it provides a framework to optimize parameters of material models (or any metamodel) to desired outcome, by minimizing the deviation of a simulation outcome to experimentally recorded data. The simulation mirrors the experiment by using the same boundaries and geometry. The experiment itself, ideally, is constructed to obtain all relevant actors changing the physical state of the sample (force, heat, etc.), as well as the state itself (displacement, strain, temperature, etc.). This procedure was shown to be especially viable for polymers with pronounced time and temperature dependent properties [67]. To numerically describe their behaviour, numerous material models with varying degrees of complexity have been developed. Again, it has been proven, that using the right instrumentation (i.e. additional digital image correlation for a standard tensile test), thereby optimized parameters are able to better predict the outcome of other, more complex systems [28, 66]. Such problems can be regarded as inverse problems, as the solution is not the response of the system, but rather the cause of the behaviour. Inverse problems often pose no analytical solution; it will be shown that the heat conduction problem considered in this work, may also be treated as an inverse problem. To solve these problems it is especially useful to acquire as much data as possible (if the model is neither overfitted nor underfitted), as the quality of predictive descriptions increases with increasing difficulty of finding a model formulation that minimizes the error over all available data [42].

Historically, computational power severely limited the value of big amounts of data. However, consider that in 1980 a top of the line consumer grade processer (Intel 8087) achieved 50 kFLOPS (50×10^3 Floating Point Operations per Second), in 2000 an Intel Pentium 4 was able to perform 6 GFLOPS (6×10^9 FLOPS), this thesis is written on a machine with an AMD Radeon RX 5700 XT GPU, that is able to crunch 8980 GFLOPS. This historic development naturally leads to an increase of people involved in data science, a term which was first shaped to its modern definition in 1992 [32]. Universities around the globe adapted and established majors in data science starting in the early 2000s, with more conservative universities playing catch up later on. The term data is famously referred to as "the oil of the 21st century" in popular culture [2], which seems like a reasonable assumption, considering there is a whole specialised industry for this field, which was already worth 189.1 billion USD in the year 2019 – and is prosperously growing [44].

One of the biggest challenges the 21st century constitutes for companies, will be to keep up with the accelerating rate of digital transformation, as technological disruptors pose an imminent threat to late adopters. One key driving factor of growth will be the ability to generate high quality data and to successfully handle big amounts of it. Moreover, discarding huge amounts of data might be considered wasteful and inefficient with the traction gaining successful adoption of ML algorithms and broadly available high-performance computing (HPC). It is unreasonable to think, that any sector will be unaffected, with some having immediate observable benefits - whereas others might still struggle to get behind the buzzwords. Especially material scientists should consider the usage of complete datasets, rather than single-point variables. Because such data is regularly generated and can be seen as a low-hanging fruit to improve available legacy methods and work on the link between chemistry, physics, geometry and macroscopic properties – in order to use existing materials to their fullest potential, and to develop new, improved materials. To prove this assumption, this thesis presents improvements to a method for measuring thermophysical material properties, based on the key principles of:

- leveraging existing data,

- improving instrumentation and

- using numerical models to get behind the physics of heat transfer.

The method concerned is known as **Laser Flash Analysis (LFA)**. It is a rather popular and broadly accepted method to determine thermal diffusivity. However, in its frequent implementation by original equipment manufacturers (OEMs), it seems to be deployed with lacklustre instrumentation, as we will show later. In combination with scarcely documented closed-source software packages, encrypted databases, that force users to work with proprietary solutions, and typically no API support; this severely limits the true potential of this method. The goal of this work is to show how this method could readily be improved to provide not only thermal diffusivity, but also thermal conductivity and volumetric heat capacity - the three most relevant thermophysical material properties. In a plea for better documentations, accessible and open software and diligent instrumentation.

1.2 THERMOPHYSICAL PROPERTIES

The terms *thermophysical* and *thermodynamic* are somewhat loosely defined with no easily observable and well posed distinctive feats to distinguish them. Therefore, thermophysical properties are further regarded to, as the subset of macroscopic material properties that are able to definitively describe thermodynamic processes. All changes to a systems internal energy (or parts thereof) over time (including the conversion between different forms of energy), or the observable change in macroscopic properties, may be considered thermodynamic processes.

Many standard literature works concerning thermodynamics in general, start by explaining the big impact this field of physics has, by giving examples of various comprehensible use cases [16, 55]. As a broad branch of physics, many different professions obviously rely on thermodynamic considerations, and arguably every engineer needs to understand the fundamentals of heat transfer. We will specifically address polymers, a class of materials that steadily attracted more research interest within this discipline, as suggested by Figure 2. Besides mainly academic considerations, with only practical implications for polymer design, chemical or physical production processes, direct applications (i.e. designing heat sensitive components) are likely to also follow this trend.
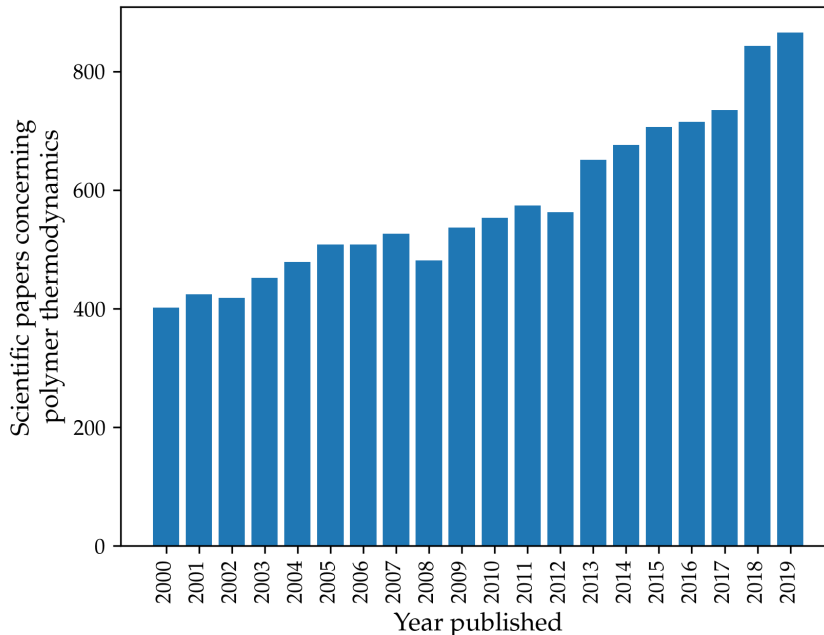

Figure 2: Increase of interest in polymer thermodynamics over time, data scraped from [1]

A big part in the increasing role of thermal considerations are, again, the advance of simulations. Due to the fact, that the governing thermodynamic equations mostly consist of differential equations (i.e. heat and mass transfer) - which are insolvable by analytical means for most real-world applications. Solutions demand numerical solvers, which profit from rising HPC availability. For polymer engineers, the simulation of production processes (injection moulding, resin curing, extrusion) is of particular interest, because of possible substantial economic benefits (discussed in 1.1). Such simulations heavily rely on the knowledge of thermophysical material data. Another contributing factor is the usage of polymers in electronics (i.e. in printed circuit boards – PCBs), as a consequence of the simplicity of production, their low cost and their insulating properties. With the sheer mass of semiconductors and electronics produced and assembled every day, designing such products using clever simulations might give any company the edge over its competition. This requires understanding the thermodynamic mechanisms in polymers and the appropriate determination of their thermophysical properties.

2

THEORETICAL BACKGROUND

2.1 THE FUNDAMENTAL LAWS OF THERMODYNAMICS

Going on further, we derive the fundamental physical definitions of necessary metrics used within this thesis, to establish deeper understanding of later presented problems. Hence, we start by providing postulates of the laws of thermodynamics.

The "zeroth law" gives hint to the historically grown definition of temperature, it was first formulated by R.H. Fowler in 1931 [16] and is more of an "afterthought" [3] than a new paradigm, developed long after the first and second law. A comprehensible definition is given by Guggenheim [41]:

> "If two systems are both in thermal equilibrium with a third system, then they are in thermal equilibrium with each other"

Whereas *thermal equilibrium* refers to an observable macroscopic state, specifically, the intrinsic property of the system: temperature. This transitive relationship further justifies mathematical descriptions of heat transfer, among other formulations.

The first law of thermodynamics considers energy as an extensive property of the system (contrary to the phenomenological temperature) and applies the concepts of energy conservation to thermodynamic processes. The statement which gave birth to the first law of thermodynamics is given by Clausius as (translated by Walter R. Brown [24]):

> "In all cases where work is produced by heat, a quantity of heat is consumed proportional to the work done; and inversely, by the expenditure of the same amount of work the same quantity of heat may be produced."

Notably, the concept in a clear definition is attributed to him, he first provided this description in an effort to describe the "force of heat" for utilisable work in steam engines in [23]. For a closed system, without transfer of matter we can write this as:

$$\Delta U = Q + W, \tag{2.1}$$

where ΔU denotes the change in internal energy of the system (a state variable), W is the work done on the system and Q is the heat transferred into the system (process variables). In simpler words: internal

energy of a system is conserved, and can only be subject to change if heat is transferred over its boarders or work is done by or on the system.

The second law introduces the concept of entropy (S) and was recognized early by Carnot, the term itself was coined Clausius and Kelvin [41, 72]. It is a term that can and has been framed under many different aspects, despite being a well-defined physical concept, the definitions are not perfectly consistent [34]. This is due to historical contingency, because the earliest formulations relied on classical mechanics and did not consider the concept of quantum states and statistical mechanics – which would be necessary for a description that can be considered correct today [87]. Entropy is always an extensive state function of the system, in order to define it, we may give a few statements that can generally be considered true for classical thermodynamic frameworks:

I For any closed system without energy transport to or from its surroundings, entropy can never decrease.

II Any non-equilibrium closed system without energy transport to or from its surroundings spontaneously approaches an entropic maximum, despite the conservation of energy inside the system.

III The entropy of a closed system in equilibrium, without energy transport to or from its surroundings, is directly proportional to the internal energy of the system.

By these statements and with the knowledge of the zeroth and first law of thermodynamics, any classical description of the second law can be matched. Take, for example the "Clausius statement" about the second law [24]:

"Heat can never pass from a colder to a warmer body without some other change, connected therewith, occurring at the same time."

Because of (III), we can identify a body of higher entropy and a body of lower entropy. As they are in contact, we view them as one system to be consistent with the above formulations. Combining the two bodies will yield a system with higher (or equal) entropy as the sum of the entropies of each body before combining them, following (I). The systems entropy will start approaching a maximum, with the total energy inside the system staying the same (II). Thus, something else has to happen inside the system that changes a state variable – remembering the zeroth law, we can directly conclude, that they need to be in thermal equilibrium. As there is no other change occurring at the same time (W=0), the bodies need to anneal their temperature

through the exchange of heat (first law).

This subset of definitions also makes it possible to distinguish between reversible ($dS = 0$) and irreversible ($dS > 0$) processes. Put this into perspective with the "Clausius theorem", about a system that absorbs an infinitesimal quantity of heat ∂Q from the surrounding with temperature T:

$$\oint \frac{\partial Q}{T} \leqslant 0. \tag{2.2}$$

This theorem, which essentially is a mathematical formulation of his statement for thermodynamic systems, is based on assuming the second law. It has since been proven true, even without those assumptions in 2011 [33]. It can be used to describe idealized reversible processes (Carnot cycle, $dS = 0$). And thus, opens a way to provide a first clear mathematical definition of entropy, within the classical thermodynamic framework:

$$dS = \frac{\partial Q}{T} \tag{2.3}$$

The third law in its most accepted form is also called the unattainability principle [57], and leads to the conclusion, that absolute zero temperature cannot be reached. This law may be more generally stated (although not true in all cases) with the words of Planck, who himself slightly rephrased a theory of Nernst (translation by the author of this thesis): "With indefinite decrease in temperature of a body of finite density its entropy approaches zero" [65]. With the entropy merely approaching zero, but never actually reaching it - as it would be impossible for any real scenario, at least by classical definitions.

These fundamental laws already incorporate the concepts of temperature, heat and entropy; we shall now find definitions that are potentially able to solve the later investigated problem.

2.2 THE STATISTICAL NATURE OF REALITY

The idea that matter is made up of smaller particles was a long disputed and controversial school of thought, even up to the early 20th century. While undoubtedly proven true today, this conception laid the groundwork for early pioneers like Bernoulli to recognize the extensive and observable properties of a gas (pressure, temperature) as a consequence of the motion of its molecules [9] – an idea which would be later described as kinetic or mechanical theory of heat [24, 83]. This led to Maxwells mechanical interpretation on collisions of perfectly elastic spheres inside a gas, developing a statistical description of the molecular behaviour - which is able to explain measurable phenomena [58]. Subsequently, L. Boltzmann recognized and refined this statistical approach, culminating in his ground-breaking definition of entropy as a form of measure for *statistical disorder* [12]. To

successfully explain why gases (or other bodies) can be made out of many small particles, but still behave as if they are single entity, it is a helpful construct to think of them as a system with a large number of constituents. Which - when observed - represent the properties of a certain macrostate (i.e. temperature), because the observer is most likely to encounter the particles in the highest multiplicity of available microstates (for temperature in gases, the according microstate would be the kinetic energy). Using gases as an example is a simple way to illustrate this. We can assume there are neglectable interaction between particles with determined degrees of freedoms (DOFs), and assume the speed of the particles (and thus their energy) follow a probability distribution. This statistical distribution was heuristically derived by Maxwell (later named Maxwell-Boltzmann distribution) in his above-mentioned work. To explain how this relates to entropy, we may consider the following thought experiment (depicted in Figure 3): A container with four distinguishable gas particles has two distinct halves. The positioning of each molecule inside the container is equally likely, the number of particles in each half is representative for a macrostate; thus, there are five achievable macrostates in total. However, as there one or more ways to distribute four particles to achieve a certain macrostate, the probability of randomly drawing a certain macrostate depends on the total number (amount) of microstates (Ω in Figure 3), that are able to construct it. Hence, not all macrostates are equal. This example is intuitively obvious, and in fact
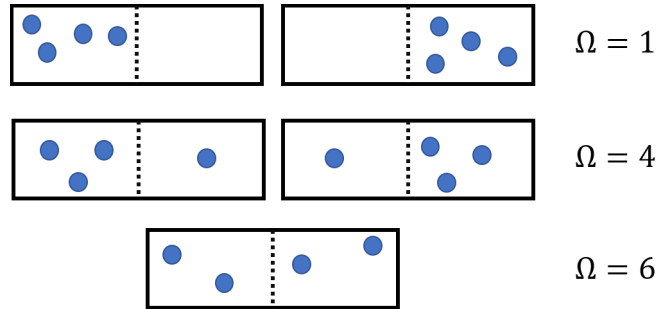
Figure 3: All possible macrostates of a system with four particles and two microstates, Ω denotes the number of possible distributions to achieve a certain macrostate

a representation of the second law of thermodynamics: entropy will approach a maximum and with it, the system will strive to maximize disorder, as we would have to apply work to keep all four particles in one half. To quantify it, we can arrange Boltzmanns formulation of entropy:

$$S = k_b \ln \Omega, \tag{2.4}$$

where the Boltzmann factor k_b is introduced, to achieve the correct thermodynamic dimension of [J/K] (as a result of the second law, see Section 2.1). The logarithmic definition is necessary as we established

entropy as an extensive system property, thereby the entropy – and, followingly, the probabilities - of two combined systems need to be additive, not multiplicative. The historical importance of this simple formula cannot be understated (today it can be found on the gravestone of Boltzmann in the Vienna Central Cemetery [34]). What Boltzmann did by defining exactly distinguishable microstates, is used today in quantum mechanics, as there are always certain allowable states of energy for every particle. It is consistent with older thermodynamic formulations, although not precisely equivalent and needs to be adopted for anything other than monoatomic gases.

In reality, every microstate is not equally possible, a more appropriate expression would be Gibbs entropy, where p_i expresses the probability of the occurrence of a microstate with energy E_i:

$$S = -k_b \sum_i p_i \ln p_i, \tag{2.5}$$

Gibbs entropy is exactly equal to earlier thermodynamic entropy formulations [47], see Equation 2.3.

2.3 WHAT IS TEMPERATURE?

Finally, we are able to provide a proper definition of temperature by using the earlier stated example about two bodies in thermal contact with one another (the outer walls are now isolated), and applying our statistical definition of entropy to it. Imagine the bodies (1 and 2) to be containers, as we did for the statistical description (but with walls to separate the particles), with a large and fixed number of gas molecules N. Each molecule is in a certain microstate, which corresponds to its kinetic energy. They are randomly moving inside the box of fixed volume V, losslessly transferring energy to one another by impact. The energy of each container is nothing but the microstate with the highest multiplicity. As already stated, we can assume the energy distribution follows a Maxwell Boltzmann distribution. The containers will again approach thermal equilibrium, the total energy is conserved: $E = E_1 + E_2 = const$. In order to count all possible microstates for total energy E, we look at the total microstates with the exact energy of E, when container one has energy E_1 and container two has energy E_2:

$$f(E_1) = \Omega_1(E_1) \times \Omega_2(E - E_1). \tag{2.6}$$

For every possible configuration (choice of E_1) the sum yields the total number of microstates: $\Omega = \sum f(E_1) = \sum \Omega_1(E_1) \times \Omega_2(E_2)$. When thermal equilibrium is reached, each box has a certain energy (not necessarily equal, thus $E_{1,eq} \neq E_{2,eq}$), which may be calculated

from the corresponding probability distribution, as the most probable macrostate is the maximum:

$$\frac{df(E_1)}{dE_1} = \frac{d\Omega_1}{dE_1}\Omega_2 + \frac{d\Omega_2}{dE_1}\Omega_1 = 0, \qquad (2.7)$$

substituting $d(E_1) = d(E - E_2)$ and rearranging yields:

$$\frac{d\Omega_1}{dE_1}\frac{1}{\Omega_1} = \frac{d\Omega_2}{dE_2}\frac{1}{\Omega_2}, \qquad (2.8)$$

which leads to:

$$\frac{d\ln\Omega_1}{dE_1} = \frac{d\ln\Omega_2}{dE_2}, \qquad (2.9)$$

In this relation, that is valid for for equilibrium systems, we now introduce Boltzmanns entropy (as in Equation 2.4), this yields:

$$\frac{dS_1}{dE_1}\big|_{N,V} = \frac{dS_2}{dE_2}\big|_{N,V}, \qquad (2.10)$$

and must satisfy $T_1 = T_2$, according to the zeroth law. We can easily see the dimension of $\frac{dS}{dE}$ must be the same as $\frac{k_b}{E}$ [1/K]. Therefore, we conclude a reciprocal relationship:

$$\frac{\partial S}{\partial U} \equiv \frac{1}{T}. \qquad (2.11)$$

Note, that we have swapped E for U, to be consistent with earlier statements about internal energy. This expression is similar to another classical thermodynamic identity, stated in Equation 2.3. The partial derivatives have been introduced to account for all possible dependencies that occur in any other setting than this thought experiment. We are now able to provide a thermodynamically correct definition of temperature in words: The change in entropy with regards to the change in internal energy of a system, is equivalent to the reciprocate of the temperature.

2.4 ABOUT HEAT

Having a clear understanding of temperature as an intensive system property, we will concern ourselves with the term heat, the various forms of heat transfer, as well as the material properties needed to describe it, with special regards to the mechanisms of heat transfer in polymers.

We already made use of the term heat while constructing the laws of thermodynamics. We might provide a simple definition thereof as given in [45]:

> "Heat transfer (or heat) is thermal energy in transit due to a spatial temperature difference."

There are different processes that can be classified as forms of heat transfer [8], we shall consider as relevant for this work the following:

- Conduction, as the diffusion of heat inside a solid or stationary fluid,

- convection, as the transfer of heat due to the movement of a fluid or gas and

- radiation, as the transmission of heat through electromagnetic waves.

The temperature inside a body can be described by the means of a field in a cartesian space $T = T(x, y, z)$, which may or may not depend on time, for transient $T = T(t)$, or respectively, steady state $T \neq T(t)$ heat transfer analysis (HTA). Common HTA problems try to calculate temperature for a given set of boundaries, to do so, we will find the governing equations. The fundamental correlation for conduction is given by J.B. Fourier [36], who found that the heat flux (thermal energy per unit area and time) inside a solid, homogeneous body, is proportional to some constant times the gradient of the temperature field:

$$\dot{q} = -\lambda \nabla T, \tag{2.12}$$

where we introduce thermal conductivity λ in [W/mK] as the proportionality factor, that is a material specific quantity which is generally dependent on temperature $\lambda = \lambda(T)$. The heat flux $\dot{q}$ is of dimension [W/m²] and also needs to be a function of space and time $\dot{q} = \dot{q}(x, y, z, t)$. The gradient is defined as

$$\nabla T = \operatorname{grad} T = \frac{\partial T}{\partial x}\hat{x} + \frac{\partial T}{\partial y}\hat{y} + \frac{\partial T}{\partial z}\hat{z}$$

and is the source of heat transfer, as stated above.

Using the first law (Equation 2.1) and treating it like an energy balance equation, we are able to construct the derivative with regards to time as:

$$\frac{dU}{dt} = \dot{Q}(t) + \dot{W}(t) . \tag{2.13}$$

The change in applied work to our body with regards to time consists of various possible different forms. For the sake of simplicity, we assume no thermodynamic work ($\dot{W}(t) = 0$), thus energy is only transferred as heat (no chemical reactions, electrical heating, change of volume, etc.).

For a solid, we may approximate the change of internal energy by disregarding the change in density ρ [kg/m³] due to temperature or pressure alterations:

$$\frac{dU}{dt} = \frac{d}{dt}\int_m u\,dm = \frac{d}{dt}\int_V u\rho\,dV = \rho\int_V \frac{du}{dt}dV . \tag{2.14}$$

To quantify the change in internal energy of any substance, we need to introduce another fundamental property of matter to link heat and temperature. As our temperature definition in Section 2.3 suggests, by adding a small amount of heat dQ ($\hat{=} dU$, without work) to a system, the system will try to maximize its entropy by occupying the newly acquired microstates. This change is proportional to the temperature. To quantify *how much* temperature changes with added heat, we introduce the heat capacity in [J/K] under constant volume as:

$$C_V(T) = \left(\frac{\partial U}{\partial T}\right)_{N,V} = \left(\frac{\partial U}{\partial S}\right)_{N,V} \left(\frac{\partial S}{\partial T}\right)_{N,V} = T\left(\frac{\partial S}{\partial T}\right)_{N,V} \; . \quad (2.15)$$

If we do not consider constant volume the last expression of above formulation can be adopted. Since we need to assume $W = 0$ we simply set $p = const$; therefore the heat capacity under constant pressure may be written as:

$$C_p(T) = T\left(\frac{\partial S}{\partial T}\right)_{N,p} \; . \quad (2.16)$$

In contrary to the extensive heat capacity C, the specific heat capacity c is an intensive system property in [J/kgK]; which is obtained by correlating specific heat of a body to its mass. The heat capacities under constant volume C_V and constant pressure C_p are related through the volumetric coefficient of thermal expansion α and the isothermal compressibility β via

$$C_p - C_V = TV\frac{\alpha^2}{\beta} \; . \quad (2.17)$$

In addition to having a practical material property to describe the amount of heat needed to change the temperature of a substance, we can clearly see why this property is closely linked to the microscopic composition of a body. Our understanding, that entropy is a function of microstates which are possible to occupy, explains why different materials have different responses to heat. Our key assumptions in Section 2.2, also enabled Dulong and Petit [29] to calculate the molar heat capacity of solids by equating the energy per mole of a substance to $3k_bTN_A$ (3 for the number of DOFs in space, N_A for Avogardos number), which leads to $C_V = 3k_bN_a$/mole= 24.94 J/mole K. This rather simple model showed to be a good approximation for elementary solids at high temperatures. Einstein [31] improved this approach by considering energies smaller than k_bT, with the use of Einstein-Bose statistics - which is necessary to describe quantum harmonic oscillators (in analogy to classical harmonic oscillators). Despite the massive impact his contribution had to the understanding of specific heat and quantum mechanics, he falsely assumed all oscillations in a solid are of the same frequency – this resulted in severe deviations for

low temperatures. Debye [27] recognised different vibrational modes, which he described as longitudinal waves inside solids. The density of states (relative number of states occupied at certain energy – "probability density over probabilities" [5]) for those modes can be seen as elementary excitations (or *quants*) for the elastic structure of our body, consisting of molecules or atoms in mechanical interaction with one another. As there are definitive vibrational modes, depending on the respective elastic interaction, this notion is often referred to as a quasi-particle; it was given the name phonon. This is a drastically better approach for calculating the molar heat capacity for lower temperatures. It only lacks accuracy for metals at low temperature, since electron movement, that was shown to contribute to heat transfer, is not considered. [73]

Regarding the discussed specific heat capacity, we can define the change in internal energy as $du = c_V(T)dT$, which we substitute in Equation 2.15 and obtain:

$$\frac{dU}{dt} = \rho \int c_v(T)dT .$$ (2.18)

Furthermore, the heat flux over our body can be calculated as:

$$\dot{Q} = -\int_A \dot{q}\hat{n}dA = -\int_V \nabla\dot{q}dV .$$ (2.19)

Combining Equation 2.13, Equation 2.18 and Equation 2.19 yields

$$\int_V \left[\rho c_v(T)\frac{\partial T}{\partial t} + \nabla\dot{q}\right] dV = 0, \text{ or}$$

$$\rho c_V \frac{\partial T}{\partial t} = -\nabla\dot{q} = \nabla[\lambda(T)\nabla T].$$ (2.20)

This partial differential equation is also known as *heat equation*. We now have a definitive relation to describe how temperature evolves throughout a body. Hence, we are able to exactly describe heat conduction by three material properties: density, specific heat capacity and thermal conductivity.

Lets assume a perfectly homogeneous body, the changes of temperature throughout the body (and over time) are small, so we may neglect the temperature dependencies of our material properties. Consequently, the term on the right of Equation 2.20 can be written as $\lambda\nabla^2 T = \lambda\triangle T$, where $\triangle$ symbols the Laplacian operator. Furthermore, it is no coincidence that the density and the specific heat capacity appear as a pair. The definition to set the specific heat capacity as energy per unit mass is purely of practical and historical reasons. Consider our earlier definition of heat capacity as a function of microscopic structure, as well as the fact that the density is nothing but mass per

unit volume - which may also be calculated/approximated as a function of molecular structure and respective molar mass. Hence, we will introduce k as "volumetric heat capacity" [J/m³K], so:

$$k = \rho c_v. \tag{2.21}$$

Note that we also got rid of the subscript V (in k, as used henceforth) for constant volume, since we assumed small temperature changes and a solid body, therefore $c_V \approx c_p \approx c$. This is a more elegant way to handle the specific heat capacity for the present case – especially since this multiplicative product is less depended on temperature, because the two factors generally behave inversely to one another (with regards to temperature). We may now rearrange our equation by dividing with c:

$$\frac{dT}{dt} = \frac{\lambda}{\rho C}\triangle T = a\triangle T, \tag{2.22}$$

where we introduced the thermal diffusivity a [mm²/s], which we may generall define as

$$a(T) = \frac{\lambda(T)}{\rho(T)c(T)} = \frac{\lambda(T)}{k(T)}. \tag{2.23}$$

The PDE in Equation 2.20 is mathematically equivalent to Fick's second law of diffusion for describing changing concentration of particles with regards to time. Diffusion is a natural and spontaneously occurring process, that equalizes differences in local concentrations due to Brownian motion – which is nothing else than another consequence of the second law of thermodynamics. Hence the name *diffusivity*. The given equation makes due with only one material property. This property can be a better variable to compare different substances. Take, for example, polytetrafluorethylen (PTFE) with a thermal conductivity of 0.24 W/mK and compare it to an styrene-butadiene (SB) Copolymer with a thermal conductivity of 0.17 W/mK. In a setting in which dimensions are constrained and temperature loads should be kept short/low, one might automatically come to the conclusion, that PTFE would be the better choice. However, due to its significantly higher density, and thus higher volumetric heat capacity, it is able to store energy better than SB. Meaning, upon receiving the same amount of heat, SB is quicker than PTFE to reach thermal equilibrium with its surrounding. This behaviour becomes clear when looking at the ratio $a_{PTFE}/a_{SB} \approx 0.92$ (material data from [49]).

Until now we have covered only conduction inside a body, for its interaction with surroundings (T_{env}), we consider the convective heat transfer of a body with surface temperature T_S by Newton's law of cooling as [45]:

$$\dot{q}_{conv} = h_{conv}(T_S - T_{env}), \qquad (2.24)$$

with the heat transfer coefficient h [W/Km²], as an average over the surface. We are assuming only natural convection, which means that there is no forced mass transfer in the immediate surrounding of our body (no air or other gas flowing over our body). The governing equations to describe natural convection are coupled, elliptic, partial differential equations [38]. This is due to the fact, that we have an evolving flow of mass by the heat that is transferred from our body to its surrounding. To reduce this complexity, there are many common approximations and an extensive framework of dimensionless parameters for various different problems to adapt and scale such simplified surrogate models. For this work we will consider [84]:

- The Nusselt number Nu as the ratio of convective to conductive heat transfer $Nu = h\bar{L}/\lambda_f$, where $\bar{L}$ is the characteristic length, which is a dimensionless quantity to describe our systems geometry in regards to convection. This in itself is subject to extensive research [52], for our later proposed problem we will consider a cylindric plate with $\bar{L} = D$. λ_f is the thermal conductivity of the surrounding fluid (in heat and mass transfer we are able to treat air as a fluid).

- The Prandtl number Pr as the ratio of momentum diffusivity to thermal diffusivity of a fluid. This leads to $Pr = \eta c_p/\lambda_f$, with η [Pa s] as the fluids dynamic viscosity.

- The Grashof number Gr as ratio of static upthrust times inertial force to the square of viscous force (all acting on the fluid) and can be defined as $Gr = g\alpha_v(T_S - T_{env})\bar{L}^3/v_f^2$, with g [m/s²] as the gravitational acceleration, α_v [1/K] as the fluids volumetric coefficient of thermal expansion and v [m²/s] as the kinematic viscosity of the fluid.

- The Rayleigh Ra number as the combination: $Ra = PrGr = (g\alpha_v)/(va_f)(T_S - T_{env})\bar{L}^3$.

There are many different (Nusselt) identities to calculate the Nusselt number from other dimensionless quantities. For our problem (natural convection) they are usually given in the form of $Nu = CRa^n$, thus we can obtain an approximation of the heat transfer coefficient for the respective case. We will consider only laminar flow n = 0.25, as well as a a plate facing downwards C = 0.25 and upwards C = 0.54 [45]. For later usage we can now write the convective heat transfer coefficient as:

$$h_{conv} = Nu\frac{\lambda}{\bar{L}} = CRa^n\frac{\lambda}{\bar{L}}. \qquad (2.25)$$

Note, that Ra contains only material properties of the surrounding fluid and the surface temperature of the interacting solid body - this will be a critical assessment later on.

The last mechanism of heat transfer which we will consider, radiation, can be described using Stefan-Boltzmann's law, which states that the thermal power (energy/time) radiated from a body is proportional to its temperature to the power of four. Stating this in terms of heat flux per surface area, if the body is fully surrounded by air with temperature T_{env} [8]:

$$\dot{q}_{rad} = \epsilon \sigma \left(T_S^4 - T_{env}^4 \right),$$

(2.26)

where ϵ [/] is the emissivity of our body and σ is the Stefan-Boltzmann constant ($\sigma = 5.670374 \times 10^{-8} W/m^2 K^4$). For small temperature differences, we can linearize this expression [8] to achieve an expression similar to Equation 2.24: $\dot{q}_{rad} = h_{rad}(T_S - T_{env})$, with an effective radiative transfer coefficient as:

$$h_{rad} = 4\epsilon \sigma \left(T_S T_{env} \right)^{\frac{3}{2}}.$$

(2.27)

2.5 HEAT IN POLYMERS

Temperature and heat have been studied long before Staudinger definitively established the concept of polymers as macromolecules [77]. The peculiar thermophysical behavior of such materials was noted as early as 1802 upon Gough discovering that rubber under tension contracts when heated. This observation was later studied by Joule and is known as the Gough-Joule-effect today [48], it is caused by "entropic elasticity", which is once again the second law of thermodynamics in effect. The rise of new concepts about the morphology of polymeric substances in the 1950s, paired with increasing understanding of thermodynamics and the explosive technological advancements at the time, inspired many researches to study thermophysical properties of polymers [39]. The link between structure and behaviour is arguably one of the most important fields of material science, as it permits the development of fundamental formulas to calculate material properties immediately if the structure is known. This knowledge is especially useful today, since modern catalysts and processes enable chemists to synthesize polymers of almost exact molecular structures.

Tarasov was first to suggest extending the established framework for the calculation of heat capacity in solids to polymeric crystals, by treating them as a continuous two-dimensional elastic chain, disregarding crystal dimensions and also interaction between chains [39]. Among others, Stockmayer and Hecht [78] improved this model with a broader evaluation of the frequency spectrum for simple

"chain polymer crystals". At the time only isothermal and adiabatic calorimetry was established, thus, such studies were severely limited as the experimental proof was not as readily obtainable. In the following years, this field flourished in unison with newer material testing methods. Today, there are various different models and approaches for the calculation of heat capacity in macromolecules [18]. To do so, they typically consider the vibrational spectrum of the solid, which is obtained by infrared (IR)/Raman spectroscopy for polymers. Other approaches use "connectivity indices" as structural descriptors [54] or even simulate the molecular dynamics [10].

To show how such a process would generally look like, C_V for polystyrene is calculated, with data from [86]. Figure 4 shows the structure of PS.
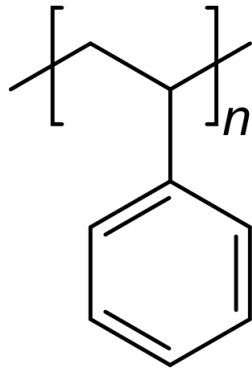

θ_E	Vibrational modes
4000	8
2000	10
1500	12
1000	8
700	2
500	1
350	1

Figure 4: Structure of Polystyrene

Table 1: Vibrational modes of PS [86]

The normal vibrational modes for the oscillating groups of PS (-CH$_2$, -phenyl, etc.) are derived and approximated from Raman spectroscopy. To calculate the energy of those modes, we will directly provide the respective Einstein temperature as $\theta_E = hf/k_b$, where h is Plancks constant and f is the frequency for the oscillators we have found. The number of modes is given for the respective θ_E in Figure 1. Furthermore, it is possible to derive that PS has 6 skeletal vibrational modes.

We use a simplified 1D Tarasov Model [35, 68, 88], which accounts for the skeletal vibrations as

$$C_T(\theta_1, \theta_3, T) = D_1\left(\frac{\theta_1}{T}\right) - \frac{\theta_3}{\theta_1}\left[D_1\left(\frac{\theta_3}{T}\right) - D_3\left(\frac{\theta_3}{T}\right)\right], \quad (2.28)$$

where θ ist the appropriate Debye temperature and D_i stands for the respective Debye function. This term can be simplified by letting $T \to 0$, expressing D as a power series and dropping θ_3:

$$C_T(\theta_1, T) = \frac{1}{3} N_A k_b \frac{\left(\frac{6.7T}{\theta_1}\right)^2}{1 + \left(\frac{6.7T}{\theta_1}\right)^2}. \tag{2.29}$$

θ_1 depends on the confirmation of the macromolecule and may be obtained experimentally with a reference measurement of C_p, or by calculating the corresponding maximum ("cutoff") frequency of wave propagation through the entire system. For polystyrene we obtain

$$C_T = 6 N_A k_b \frac{\left(\frac{T}{42.5}\right)^2}{1 + \left(\frac{T}{42.5}\right)^2}. \tag{2.30}$$

To account for group vibrations, we use Einsteins definition for the heat capacity of solids:

$$C_E = N_A k_b \sum n_E E \left(\frac{\theta_E}{T}\right), \tag{2.31}$$

with n_E denoting the number of modes with energy E of

$$E \left(\frac{\theta}{T}\right) = \frac{\left(\frac{\theta}{T}\right)^2 \exp\{\frac{\theta}{T}\}}{\left(\exp\{\frac{\theta}{T}\} - 1\right)^2}. \tag{2.32}$$

Finally, we obtain C_V by adding the contributions of skeletal and group vibrations. The result is compared to experimental values for C_p [37] and depicted in Figure 5.
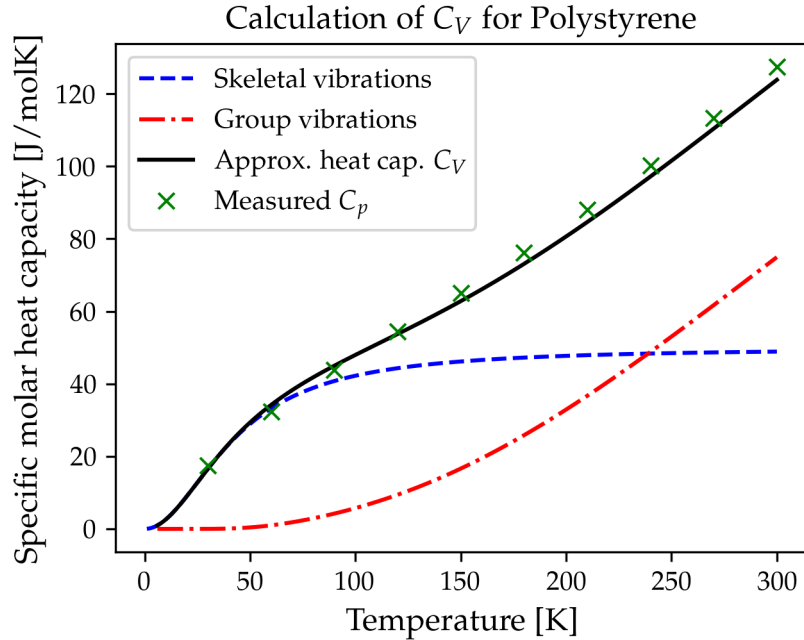

Figure 5: Calculated specific molar heat capacity of PS compared to measured values [37]

As shown for an amorphous polymer, even such simple models yield reasonably accurate descriptions in broad temperature domains. Obviously, when approaching glass transition temperatures (or phase changes at melting temperature) this simple model will fail, as other factors - such as free volume - have to be considered. For higher temperatures C_p and C_V will diverge, as specific volume increases if a sample is allowed to expand.

Understandably, thermal conductivity - just as heat capacity - is a function of morphology. The main difference in these two properties is, that conductivity considers heat fluxes, rather than just the quantity of heat. This leads to the question "how fast is heat travelling through a body". In Section 2.4 we already established the term phonon as a quasiparticle, which obeys Bose-Einstein statistics. For the sake of simplicity we introduce the mean speed of a phonon as $\bar{c}$; and $\bar{l}$, as the mean free path the phonon is able to travel unhindered through the solid. By the notion of particles with certain speeds and energies, the thermal conductivity of a substance may be derived in the same way as it is possible for gases in the kinetic theory of gases. This was done by Debye [27] and leads to [81]:

$$\lambda = \frac{1}{3}C(T)\bar{c}\bar{l},\qquad(2.33)$$

where $C(T)$ stands for the specific molar and volumetric heat capacity. This approach significantly overestimates the conductivity even for perfect crystals, as shown by Berman [70], as any real crystal will contain various imperfections. The fact that phonon transfer is path dependent explains why there is no definitive and practically useful approach to calculate thermal conductivities for many dielectric substances (aside from molecular dynamics simulations). Especially, for polymers or polymer composites with highly disordered phases, influencing factors (i.e. crystallinity and crystal orientation; cross-link density, type and length; fillers, filler geometry and orientation; molecular weight and distriburion; inherent density distributions etc.) can be identified and materials may be accordingly optimized [21, 51, 61, 82, 89]. However, meaningful calculations are often cumbersome. Hence, at least hitherto, it is best directly determined.

2.6 EXTRACTING MATERIAL PROPERTIES

As the necessary fundamentals of heat and heat transfer have been covered, the question arises on how those describing material properties are obtained. Following, we will provide the concepts, and explain the details, of the methods used in this thesis.

The first property of interest is density ρ. As stated earlier, density is mass per unit volume, for unfilled polymers it is typically given in [g/cm³] and ranges anywhere from 0.8 (low semi-crystalline or amorphous thermoplastics; elastomers) to 2.3 g/cm³ (highly semi-crystalline thermoplastics, thermosets) at room temperature. The measurement methods for solids are based on Archimedes' principle: the upthrust of a solid, that is fully immersed in a fluid, is equivalent to the weight of displaced fluid. By the knowledge of the fluids density alone (titration) or the fluids density as well as the samples weight immersed and not immersed in the fluid ("immersion method" - hydrostatic weighing) or the fluids density as well as the samples weight and the weight of the displaced fluid (pycnometry), the density of the sample can be calculated. In this thesis hydrostatic weighing will be used in accordance to DIN EN ISO 1183.

The determination of heat capacities is carried out by measuring the response of system (change in state variables) under specific constraints due to defined incremental conditional changes (thermal, volumetric, heat, heat flow, pressure, chemical processes, etc.). Adiabatic calorimetry (adiabatic meaning no heat transfer through the systems boundaries) is one of the oldest, yet still the most precise approach for the acquisition of heat capacity [46]. In this method, the sample is shielded from its surroundings - thus referred to as adiabatic - the temperature is equilibrated and then the sample is subjected to a defined amount of heat – after which the equilibrium temperature is measured. The specific heat capacity is calculated as $c_p = Q/m\Delta T$. Adiabatic boundaries generally require lavish isolations. Also the time it takes for the system to reach equilibrium at every stage results in lengthy measurements. To tackle this issue, differential scanning calorimetry (DSC) was established in the 1960s [85]. It allows to continuously measure (hence "scanning") the thermodynamic response of small quantities, generally only a few milligrams, of a substance [88]. There are different implementations of this method, this work will use the heat flux approach. For this method, the sample is put into an aluminium crucible. Additionally, an empty aluminium crucible is used as a reference. Both are put into one test chamber (furnace) and are subjected to an equal heat flux. The heating or cooling rate is predetermined by a temperature profile, that is exercised upon the reference crucible. The temperature of both cru-

cibles is measured, as the sample crucible contains a substance that also "absorbs" heat, a difference in temperature (hence "differential") is recorded, which is proportional to the change in internal energy. Thus, we can state:

$$\frac{\dot{Q}}{m} = \frac{dT}{dt} c_p \tag{2.34}$$

This heat flow per mass substance is then provided as a function of temperature or time. To obtain the specific heat capacity under constant pressure we:

1. Measure an empty (emp) crucible to obtain a baseline for our oven (technical correction)

2. Measure a reference (ref) substance with precisely known c_p (physical calibration)

3. Measure our sample (sam) and calculate c_p as:

$$c_{p,samp} = c_{p,ref} \frac{m_{ref}(\dot{Q}_{sam} - \dot{Q}_{emp})}{m_{sam}(\dot{Q}_{ref} - \dot{Q}_{emp})}. \tag{2.35}$$

The DSC is a powerful method to evaluate polymer samples, as its best suited for the relevant temperature ranges. Additionally, it is quick, reasonably accurate, makes due with small samples, measures continuously and can give clues about physical condition and chemical composition [30].

The acquisition of thermal conductivities is carried out under two substantially different aspects: by steady state or transient methods. Just as the name discloses, steady state measurements require thermal equilibrium, which is reached after a controlled heat flux is consistently imposed upon the sample. Knowing the magnitude of the heat flux and measuring the temperature gradient of the sample, enables the tester to use Fourier's law in its simplest form. Imaginably, those measurements are straight forward, easy to understand and generally require only inexpensive equipment. The difficulties lie in controlling the system (ideally adiabatic) and having exact sample dimensions of sufficient size. If done correctly those methods still are considered the most precise measurements, the obvious shortcomings are, that all of those methods are slow and barely automatable. For this work, a Guarded Heat Flow Meter (GHFM) is used, corresponding to ASTM E1530 – in this method the sample is pneumatically squeezed in between two plates of certain temperatures (one heated, the other cooled; controlled with heat sinks and Peltier elements) and the heat flux is recorded with appropriate transducers.

Transient methods are based on momentary responses and do not require the system to reach equilibrium. As we can see in Equation 2.20, this obligates us to find solutions for this parabolic PDE, because the term on the left has to be regarded. Hence, the mathematical models are more complex and the experimental set-up tends to be more difficult, as simplifying boundaries may need to be fulfilled. Because there are many different ways to state this problem, there are various established methods to solve it: transient hot wire, 3-ω method, transient plane source, amongst others. Their common advantage over steady state measurements is, that they are magnitudes faster. One method that is frequently used to measure thermal diffusivity, and subsequently derive thermal conductivity, is the the Laser Flash method or Laser Flash Analysis (LFA). It was introduced by Parker in the 1960s [64] and quickly gained popularity, because it enabled very fast measurements from as low as -120 °C, up to 2800 °C (with a few later omissions). This method also opens pathways to automate the measurement, due to its inherently contact-free nature. It is considered especially viable for highly conductive (or rather diffusive) samples, but permits accurate measurements of insulators with diffusivities of 0.01 mm²/s. It showed to be a suitable method for polymers [17, 50].

Figure 6 schematically shows the experimental setup for LFA measurements. The sample is subjected to a heat pulse (q_0), that is introduced by the flash lamp, the systems response is captured by the measurement of the surface temperature on the opposing site. Parker disregards in-plane heat flow $T = T(x, t)$, with $0 < x < L$, assumes perfect insulation (adiabatic boundaries) and a sample of uniform
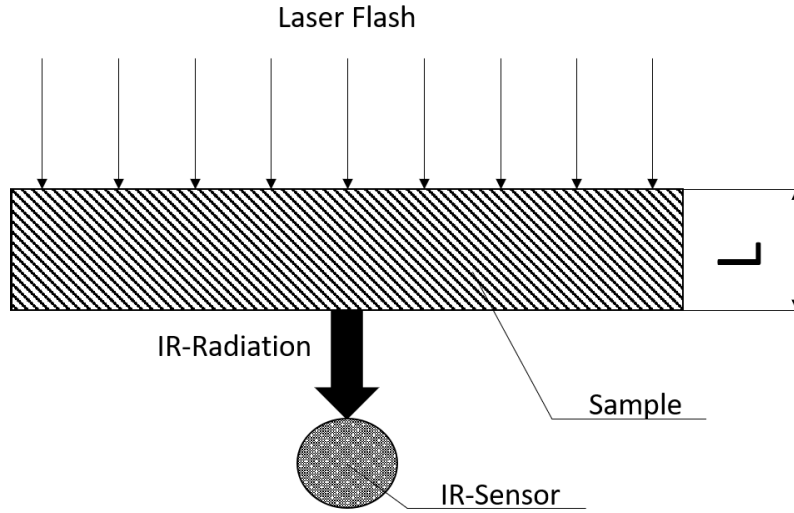
Figure 6: Experimental setup for laser flash analysis, schematic illustration obtained from [71]

thickness L, as well as known temperature distribution for $t = 0$ and an instantaneous absorption of the laser pulse directly within the thickness g. These simplifications lead to following solution of Equation 2.22 (as given by [15]):

$$T(x,t) = \frac{1}{L} \int_0^L T(x,0)dx + \frac{2}{L} \sum_{n=1}^{\infty} \exp\left\{\frac{-n^2\pi^2 \alpha t}{L^2}\right\}$$

$$\times \cos\left(\frac{n\pi x}{L}\right) \int_0^L T(x,0) \cos\left(\frac{n\pi x}{L}\right) dx. \quad (2.36)$$

With (k as defined in Equation 2.21)

$$T(x,0) = \frac{q_0}{kg} \text{ for } 0 < x < g, \text{ and}$$

$$T(x,0) = 0 \text{ for } g < x < L, \text{ thus:}$$

$$T(x,t) = \frac{Q}{kL}\left[1 + 2\sum_{n=1}^{\infty} \cos\left(\frac{n\pi x}{L}\right)\frac{\sin(n\pi g/L)}{n\pi g/L}\right.$$

$$\left. \times \exp\left\{\frac{-n^2\pi^2 \alpha t}{L^2}\right\}\right]. \quad (2.37)$$

Because $g \ll 1$, $\sin(n\pi g/L) = n\pi g/L$. Therefore, we can write the temperature evolution on the rear surface ($x = L$) as

$$T(L,t) = \frac{Q}{kL}\left[1 + 2\sum_{n=1}^{\infty} (-1)^n \exp\left\{\frac{-n^2\pi^2 \alpha t}{L^2}\right\}\right]. \quad (2.38)$$

Defining two dimensionless parameters: the dimensionless temperature $V(L, t) = T(L, t)/T_{max}$, with T_{max} as the maximum rear surface temperature; and $\omega = \pi^2 a t/L^2$ as the dimensionless time, we may write this as

$$V(L, t) = 1 + 2 \sum_{n=1}^{\infty} (-1)^n \exp\{-n^2 \omega\}. \tag{2.39}$$

This formulation allows us to make general statements, which can be applied for any dimension or material. Figure 7 shows the rise of the dimensionless temperature V on the rear surface of our sample as of Equation 2.39.
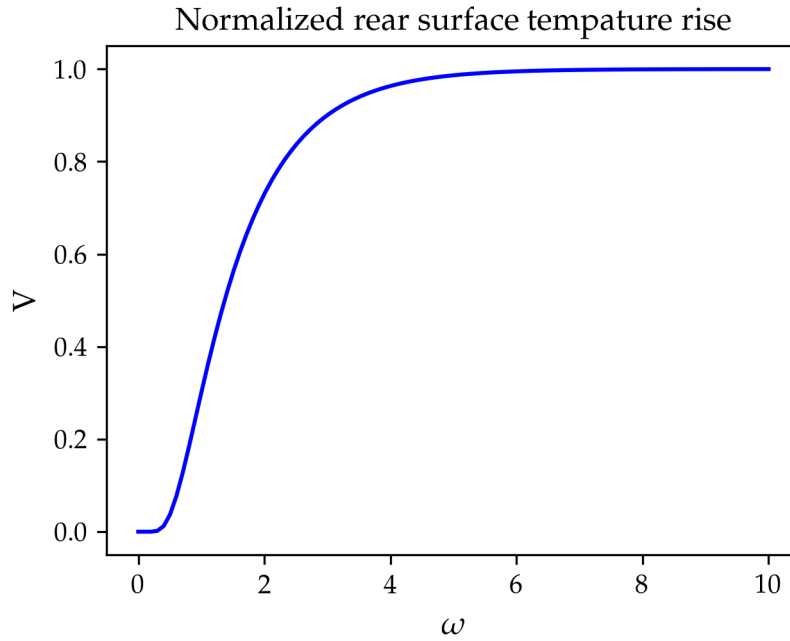

Figure 7: The adiabatic solution to the underlying problem within standard laser flash analysis

Finally, we can state when $V = 0.5$, $\omega \approx 1.38$. This leads us to a solution in only one material specific variable:

$$a = 1.38 L^2/\pi^2 t_{0.5}, \tag{2.40}$$

with $t_{0.5}$ as the time it takes our sample to reach the half of its maximum temperature. This clever formulation lets us obtain the diffusivity without knowing the exact temperature (just the curve over time is needed, the sensor does not even have to be calibrated), or the exact heat input.

In order to match basic assumptions for this adiabatic approach, the duration of the measurement has to be short enough to keep the losses through radiation and convection neglectable. This means, that either the sample has to be thin, or the diffusivity has to be high. The solution would fail for an inhomogeneous sample, such as composites with higher in plane diffusivities due to the incorporation of fibres - as this would lead to unaccounted "conductive losses". Furthermore, we assume an infinitesimal short pulse/heat flux, that immediately results in a temperature rise in a very small section of our material – this is obviously technically impossible; thus, we have to deploy mitigation strategies. For one, we have to use rather expensive pulsed laser flash lamps. Furthermore, as we introduce heat through radiation, we would need to consider the optical properties of our substance (absorptivity, reflectivity, transmissivity; respectively emissivity). To circumvent this, we coat the sample with a thin layer of graphite flakes. By doing so, a black body is imitated - in both directions, as the infrared sensor also relies on good emissivity within its recorded wavelength to produce evaluable signals with low noise.

Over the years many suggestions based on analytical optimizations have been made to ease the limitations of the original Parker model. One of the most important improvement was proposed by Cape and Lehman in 1963 [14], who accounted for radiative heat losses on both surfaces and the outer walls of a cylindric sample, as well as the pulse shape and duration. Their analytical solution leads to following expression for the rear surface temperature as a function of radial position, under the premise of a uniform flux, which is absorbed in a very thin surface layer:

$$
T(r, t) = T_0 + \frac{q_0}{\lambda} \sum_{m=0}^{\infty} C_m X_m \sum_{i=0}^{\infty} D_i(r, Y_r)
$$
$$
\times \int_0^t d\tau\, W(\tau) \exp\{\omega_{im}(t - \tau)/t_c\}, \quad (2.41)
$$

in which they defined t_c as the characteristic time:

$$
t_c = \frac{aL^2}{\pi^2}, \quad (2.42)
$$

τ as the pulse length, $W(\tau)$ as a function to characterize the pulse shape, with the C_m as

$$
C_m = (2a/L)(-1)^m X_m (X_m^2 + 2Y_x + Y_x^2)^{-1}, \quad (2.43)
$$

and X_m as the roots of

$$
X_m = (X_m^2 - Y_x^2) \tan X_m = 2X_m Y_x, \quad (2.44)
$$

where Y_x characterizes the heat loss through linearization of Stefan-Boltzmanns law (similiar to Equation 2.27) as:

$$Y_x = 4\sigma\epsilon T_0^3 \lambda^{-1} L, \tag{2.45}$$

and Y_r for the radiative heat losses through the outer walls as

$$Y_r = 4\sigma\epsilon T_0^3 \lambda^{-1} r_0, \tag{2.46}$$

where r_0 is the sample radius. Furthermore, ω_{im} is defined as

$$\omega_{im} = -(L/\pi)^2 (X_m^2/a^2 + z_i^2/r_0^2), \tag{2.47}$$

where z_i are the positive roots of

$$Y_r J_0(z_i) = z_i J_1(z_i), \tag{2.48}$$

with J as the zeroth and respectively first order Bessel functions. And finally D_i as

$$D_i(r, Y_r) = [2Y_r/(Y_r^2 + z_i^2)] J_0(z_i r/r_0)/J_0(z_i). \tag{2.49}$$

Ultimately, we can calculate thermal diffusivity by

$$a = \frac{t_{0.5}}{t_c} \frac{L^2}{pi^2 t_{0.5}}. \tag{2.50}$$

For this approach to function, some polynomials have to be solved numerically (namely z_i for Y_r and X_m for Y_x), Cape and Lehmann gave approximate solutions and equations in their work to speed up this process. Later those approximations have been improved mathematically (i.e. [11]). It is perhaps the most used LFA evaluation method today, as its not only available within the software of the relevant OEMs, but also the typically recommended evaluation approach.

Another, albeit more corrective, improvement is to not merely rely on the "half-time-rise" for the calculation of a, but to use more data points throughout the normalized curve. Heat loss models slightly shift the normalized half time to earlier times ($t_{0.5}/t_c$ decreases with increase in Y, as already noted by Cape and Lehman [14]). t_c is not known a priori, hence a better solution is given by Clark III [22], who divided t/t_c at higher percent rises by t/t_c at lower percent rises to eliminate t_c and plot those ratios as a function of t_c. This is also experimentally more viable, as we might now obtain the times at any two proposed normalized temperature increases, say 0.8 and 0.2, and look at the plot of the ratios (or use proven existing polynomial fits) to obtain the corrected $a\, t_{0.5}/l^2$.

Several other approaches to account for heat losses [26], finite pulse time [4] or optical properties of the material [59, 60] have been published. Newer methods for the general calculation used logarithmic transformations [79] or found other analytical solutions to the underlying HTA problem within the Laplace domain ([19]. It has been used to estimate thermal contact resistance [62], or to characterize layered and composite structures [20, 69]. A sector that did not get too much attention is the possibility to determine specific volumetric heat capacity alongside thermal diffusivity to simultaneously derive thermal conductivity. However, eliminating the need for additional density and heat capacity measurements, makes a lot of sense for rapid and automated property determinations (i.e. alongside material manufacturing). Many researches seem to mostly fit the heat loss by optimizing dimensionless quantities, as to not touch thermal conductivity. Very few [53, 74] seem to notice and elaborate on the practical implication of the possibility to directly obtain multiple parameters. We will try to find efficient ways to do so in the following section.

REFINING THE MEASUREMENT METHOD

3.1 PROBLEM DEFINITION

In order to obtain thermal conductivity λ in a laser flash experiment, we could try to determine the volumetric heat capacity k and rearrange Equation 2.23. This is possible if we were able to determine the energy (heat) input of the laser. We can generally state, that

$$Q = \Delta T m c = \Delta T V \rho c = \Delta T A L k = q_0 A,$$

with ΔT as the maximum temperature increase on the rear surface. Thus we can obtain k as:

$$k = \frac{q_0}{\Delta T L}. \tag{3.1}$$

This rather simplistic approach can be sufficient, as we will show later. However, since the surface heat flux introduced by the laser pulse is usually not readily obtainable, it would be beneficial to find technical solutions around it (proposed in Section 3.2) or to exclude/determine it (Section 3.3 & Section 3.4).

As the materials diffusivity is known after the fact, and the temperature response curve is recorded, the search for the heat flux (or other thermophysical properties) can be seen as an inverse problem. As early as 1966, J.V. Beck [6], who greatly contributed to inverse heat transfer problems in general, investigated possibilities to simultaneously estimate both k and λ for transient heat experiments. The rear surface temperature $T_{S,2}$ of our sample is generally a non linear (parabolic) function of k and λ (see Equation 2.20), we may want to approximate a solution by Taylor-series expansion to iteratively approach the experimental temperature history:

$$T(k, \lambda) \approx T_{k_0, \lambda_0} + \frac{\partial T(k, \lambda)}{\partial k}\Big|_{k_0, \lambda_0} \Delta k + \frac{\partial T(k, \lambda)}{\partial \lambda}\Big|_{k_0, \lambda_0} \Delta \lambda \tag{3.2}$$

It can be shown that if the temperature is given at both boundaries, or one or both boundaries are insulated, the thermal properties can not be determined [7], because it would yield a linearly dependant relation of $k T_k + \lambda T_\lambda = 0$. Hence, we need to change our experiment or introduce other nexuses. Either way, there are plenty methods and approaches within the toolset of inverse engineering, that are potentially able to deal with such problems [25]. We will demonstrate a simple approach in Section 3.3.

3.2 IMPROVING INSTRUMENTATION

The commercial LFA apparatus, that is in operation at Polymer Competence Center Leoben GmbH (specified in Chapter 4), is not equipped to provide definitive temperature measurements. As clarified in Chapter 2, it does not need to, since we are only interested in the normalized curve to determine the characteristic time for a. It does however, contain a method within the software to obtain c_p. This is possible by conducting a reference measurement on a known substance with defined thermophysical properties and geometry, and relating it to a sample with known density and geometry. The voltage signal for the temperature and the flash lamp is known and proportional to the respective physical quantity, hence c_p can easily be acquired. This requires at least two manual measurements and since the lamp characteristics change over time (due to degradation), the reference measurement has to be carried out ideally right before or after the sample measurement. A big role in the accuracy of this procedure is also the placing of the samples inside the apparatus, since it has multiple sample holders, which are accessed individually by the motorized IR sensor above. The samples inside the thermally controlled testing chamber are kept in between glass insulators with appropriate optical properties. These glass shields are prone to collect dirt from the graphite coating of the samples, or grease from the user changing the samples, naturally this introduces another source of error for relational measurements. Furthermore, by only relatively comparing reference to sample material, the optical properties of the two substances need to be similar, as well as their geometry and thermophysical properties; otherwise the heat losses would not be comparable. The procedure could be automated and improved as follows:

Let the sensor above be fixed and place the samples on a rotary table inside the testing chamber - such that there is exactly one position for the experiment. Include a fixed spot on the table for a reference material (could be graphite to mimic the optical properties of the coating, preferably not directly accessible and guarded throughout the measurement). Since the chamber itself is already thermally regulated, the IR-sensor can be easily and accurately calibrated by executing a temperature program on the precisely known reference material. Thus, we may now automatically determine the energy of the laser with a shot at our reference material.

Other conceivable improvements may regard the flash lamp (optimize wave length) or the sensor (introduce another dimension through 2D thermography for anistropic materials). To make a point for the viability of true physical measurements (temperature), we used a ther-

mocouple on a reference material inside the apparatus to calibrate the IR-sensor and the flash-lamp. See Chapter 4.

3.3 NUMERICAL MODEL

If the energy of the heat flux is not known, the calculation of other material properties is not as straight forward. To obtain other material properties, and to further underline the benefit of calibrated temperature measurements, the principles of inverse engineering are exploited to find a solution. Consider a model of the physical situation as illustrated in Figure 8. This model can be described by following equation (see Equation 2.20):

$$k\frac{\partial T}{\partial t} = \lambda\frac{\partial^2 T}{\partial x^2} \qquad (3.3)$$

with the boundary conditions due to the applied heat flux and losses (see Equation 2.12 & Equation 2.24):

$$-\lambda\frac{\partial T}{\partial t}\Big|_{x=0} = \dot{q}_0(t) - \dot{q}_{conv} - \dot{q}_{rad}$$

for convenience we define $h = h_{conv} + h_{rad}$.

$$-\lambda\frac{\partial T}{\partial t}\Big|_{x=0} = \dot{q}_0(t) - h(T_{x=0} - T_\infty) \qquad (3.4)$$

$$-\lambda\frac{\delta T}{\delta t}\Big|_{x=L} = -h(T_{x=L} - T_\infty) \qquad (3.5)$$

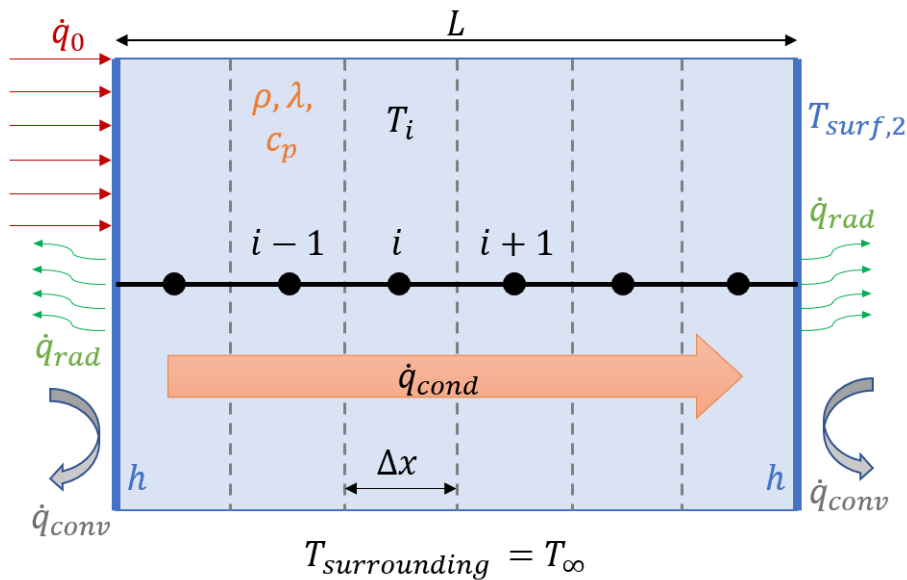With $0 \leqslant x \leqslant L$ and $T(x, t = 0) = T_0$.

Figure 8: Discretized model of a sample during LFA measurements

To find a solution, we assume our body is a one dimensional rod with n nodes, where each node represents the volume fraction $\propto \Delta x/L$, as $L = \mathrm{const}$. We can express the change in energy inside the ith node as caused by conductive heat transport as follows:

$$\Delta E = E_{in} - E_{out}$$

$$k\frac{dT_i}{dt}\Delta x = \dot{q}_{in}|_x - \dot{q}_{out}|_{x+\Delta x}$$

$$k\frac{dT_i}{dt}\Delta x = -\lambda\frac{dT}{dx}\Big|_x + \lambda\frac{dT}{dx}\Big|_{x+\Delta x}$$

$$k\frac{dT_i}{dt}\Delta x \approx -\lambda\frac{T_i - T_{i-1}}{\Delta x} + \lambda\frac{T_{i+1} - T_i}{\Delta x}$$

$$\frac{dT_i}{dt} \approx a\frac{T_{i+1} - 2T_i + T_{i-1}}{\Delta x^2} \tag{3.6}$$

And so, we derived the forward Euler method (finite difference approximation) through physical considerations - which poses a solution for the heat conduction equation, because

$$\lim_{\Delta x \to 0} a\frac{T_{i+1} - 2T_i + T_{i-1}}{\Delta x^2} = a\frac{\partial^2 T}{\partial x^2} = \frac{\partial T}{\partial t}. \tag{3.7}$$

Thus, we are able to obtain the temperature of node i with the approximation:

$$T_i(t + \Delta t) \approx T_i(t) + \frac{dT_i}{dt}\Big|_t \Delta t. \tag{3.8}$$

Heat losses will be considered in the first node with

$$\frac{dT_{i=1}}{dt} \approx a\frac{T_{i+1} - T_i}{\Delta x^2} + \frac{1}{k\Delta x}[q_0(t) - h(T_1 - T_\infty)], \tag{3.9}$$

and in the last node as

$$\frac{dT_{i=n}}{dt} \approx a\frac{T_i - T_{i-1}}{\Delta x^2} - \frac{1}{k\Delta x}h(T_n - T_\infty). \tag{3.10}$$

Since our definition of h leads to a function that is not directly dependent on k or λ of our solid, we achieved a system in which k and λ are not linearly dependant on one other, but still linked through $\lambda = ak$. Hence we are able to retrieve both values by minimizing

$$S(a, k) = \int_{t=0}^{t_{end}} [T_{surf,2}(t) - T_{i=n}(t)]^2 dt, \tag{3.11}$$

where $T_{surf,2}$ are the experimentally obtained values. There are different algorithms to guess and optimize such minimization approaches which could be used to elegantly find a solution, but since we want to merely show the validity of this procedure we will brute force it to

find a reasonably accurate approximation. To limit this approach, we use a reasonable range of k for polymers. This is better than choosing a range for λ, because it does not change as much with temperature and varies less from polymer to polymer (discussed in Section 2.4). Furthermore, the shape of the pulse is obtained by the voltage drop U(t) on the flash lamp as a function of time. In order to link it to a physical quantity, we normalize it and multiply it by the energy the sample were to receive under our first estimate for k and the recorded temperature rise ΔT (see Equation 3.1), so:

$$\dot{q}_0(t) = \frac{U(t)}{\int_t U(T) dt} * q_0 \tag{3.12}$$

However, since we are considering heat losses, the adiabatic definition of q_0 would underestimate the actual heat flux, resulting in a lower maximum temperature. Therefore we will need to correct this term, ideally by finding a relationship between the heat flux and the maximum temperature rise, under the consideration of changing heat transfer coefficients. To do so, we will simulate this experiment as described for a range of q_0, which arise as a result of our initial guesses for k. Thus we will obtain the maximum temperature and plot it in relation to the measured maximum temperature over the respective energy. This correction term is then accounted for, by adapting Equation 3.1, through multiplying the maximum temperature with the reciprocate of our correction term, to increase the maximum temperature in order to match the experimental maximum temperature. In essence, we increase the heat flux energy to appropriate levels, without changing material properties. Afterwards we will simulate the experiment for each corrected energy to acquire the best fit (by least mean square error), which should yield a best guess for k and therefore also λ. This is possible, because we first correct the respective heat flux to match the maximum temperature, and only then scan for the material properties which would result in the curve shape we obtained experimentally. We do not fit heat losses, but obtain an approximation for them based on appropriate physical relations.

To explicitly demonstrate how this procedure works, we will show it step by step for a single laser shot on an polybutylene-terephthalate (PBT) sample. First we obtain the thermal diffusivity through any established method, for example the model of Blumm [11] (with fitted heat losses, baseline and pulse correction) as featured in the software package Proteus® (NETZSCH-Gerätebau GmbH, Selb, Germany), this yields a reasonable $a = 0.142 mm^2/s$. The pulse shape is obtained and shown in Figure 9. Because our calculations rely on a discrete step time, we could approximate the shape by nearing Δt to the acquisition time of the voltage signal, and apply the relative amount of q_0 at each increment. However, since we used the interpreted programming language Python, and did not optimize the code, we need to

mind the computational efficiency of our method. Therefore, we will use a step time which is equal to the pulse duration (in this case 1.5 ms), so the corresponding heat flux is fully applied within the first step.
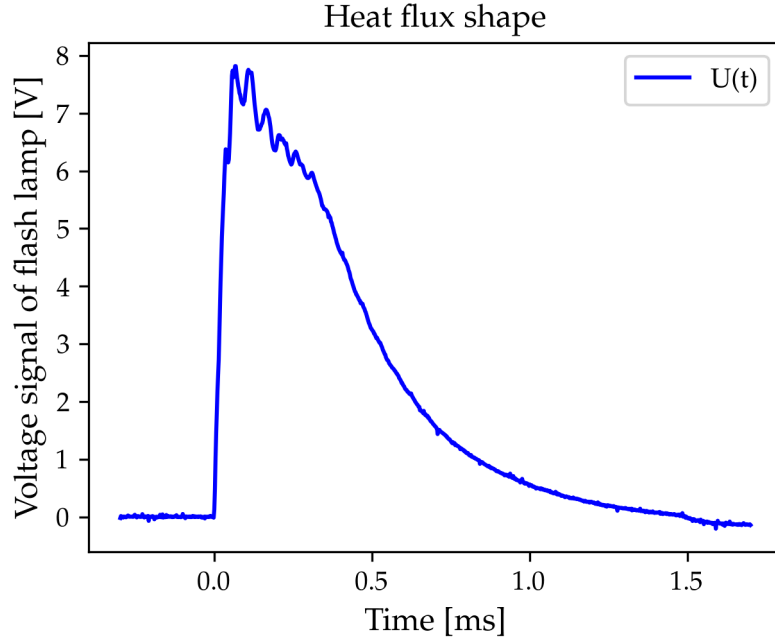

Figure 9: Pulse shape of the flash lamp during the PBT measurement

The temperature response curve is calculated based on our calibration of the IR-sensor (see Section 4.3). For convenience we fitted a spline through the data points to match our step time for later usage, shown in Figure 10.

Next we obtain the necessary relationship for our correction term. We do so, by calculating ten different energies in the appropriate k range for polymers (1.2 - 2.2 J/cm³K) using $\Delta T_{measured} = T_{max,meas.} - T_{min,meas.}$ in Equation 3.1; and letting those energies, as well as k, be the parameters of the simulation to compute the reduced T_{max}. The heat transfer coefficient is calculated continuously, as it is dependent on the surface temperature of our material. The sample is inside a heated chamber at 30°C, thus we use literature values for the surrounding fluid (thermophysical properties of air at 300 K from [45] and the coefficient of thermal expansion from [84]). The result for our correction factor is plotted in Figure 11.

Finally we are able to fit the curve of our simulation by varying k and calculating $q_{0,corr}$ for each guess in our range. This could be optimized as mentioned above, we will use the same ten k values as we did earlier and compare the mean square error. Thus we are able
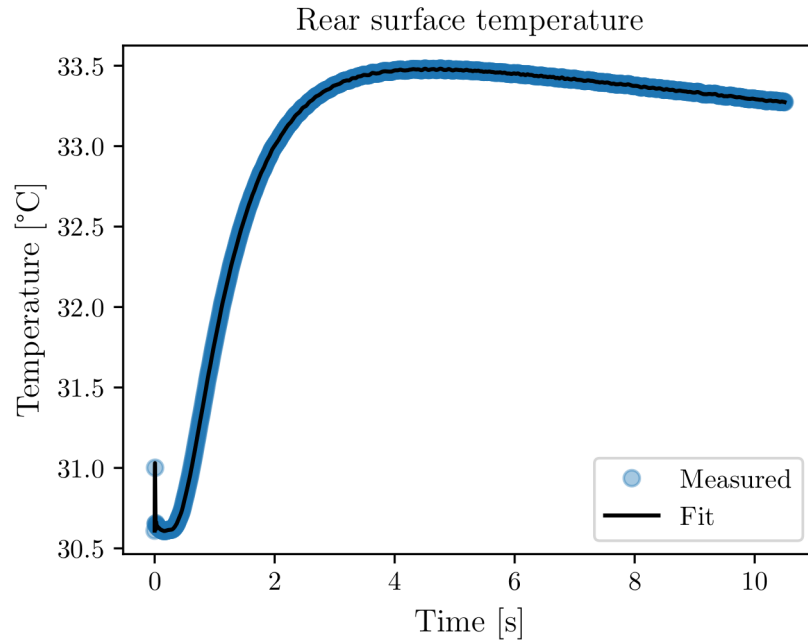
Rear surface temperature

Figure 10: Calibrated temperature response curve

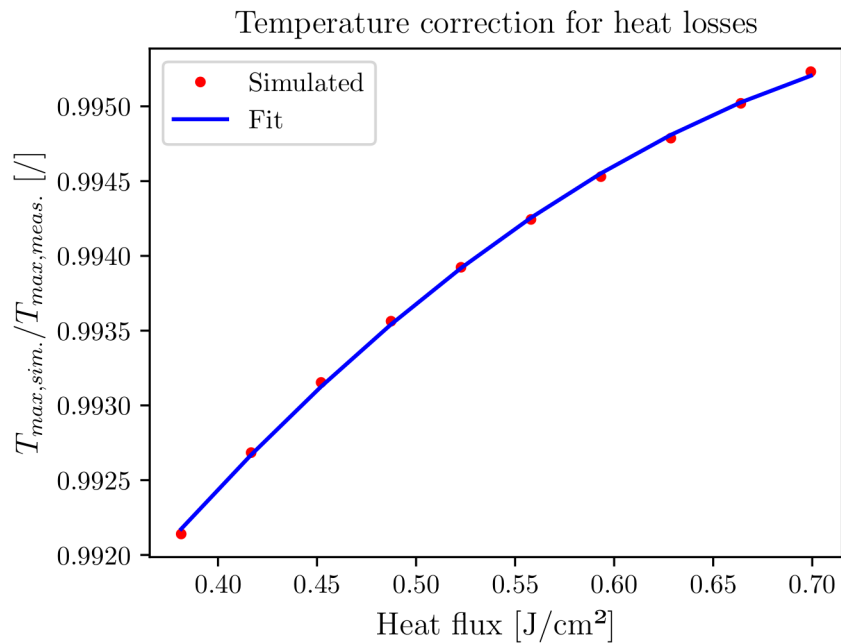Temperature correction for heat losses

Figure 11: Correction of the maximum temperature rise to account for heat losses

to roughly determine the area of local minima. This is illustrated in Figure 12. The final result of our rear surface temperature simulation is compared to the measured data in Figure 13
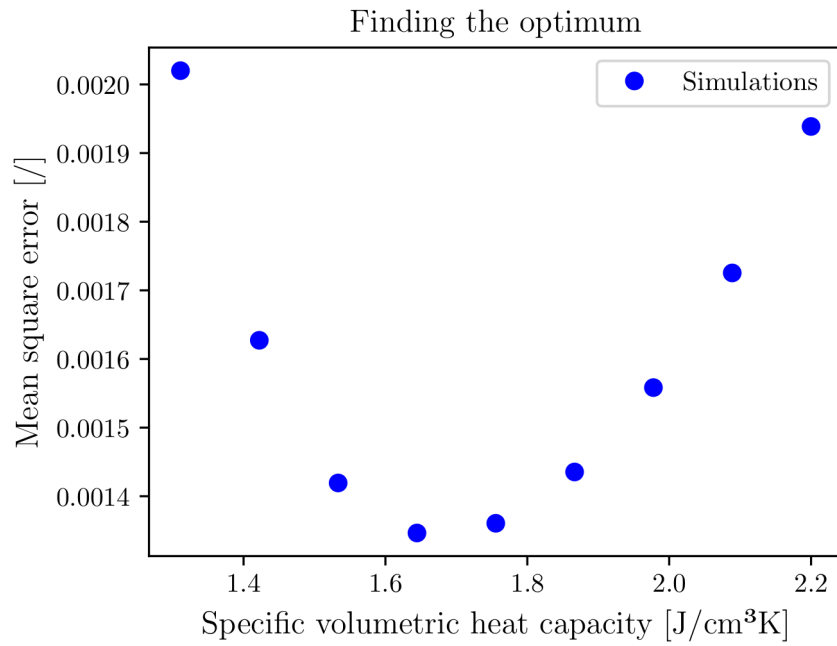
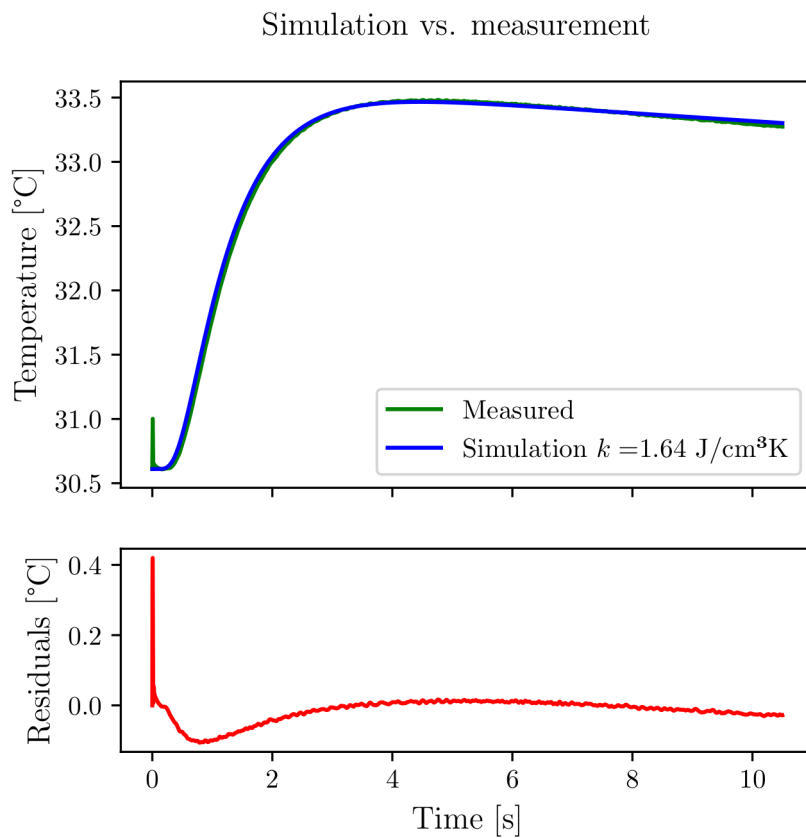**Figure 12:** Finding the optimum k that minimizes the simulation error

Figure 13: Resulting simulation of our best guess for k with residuals

Thus, we inverse engineered $k = 1.64$ J/cm³K (compared to 1.68 J/cm³K calculated by multiplication of measured values ρ & c_p as given later in Chapter 5), with $\alpha = 0.142$ we get a $\lambda = 0.233W/mK$ (compared to 0.249 W/mK measured). The principle was made clear, obviously there are many possible improvements. As Lunev [56] rightly stated with the title of his work: complexity matters. To improve it, we may account for optical properties of our substance (the reason why the first measurement point is heightened), use a multidimensional model and introduce other factors such as graphite coating, irradiated spot size, thermal contact to the sample holder, use the exact pulse time, etc.

3.4 DISCUSSING OTHER POSSIBILITIES

To make use of the discussion about entropy, statistics and thermophysical properties of polymers - we want to briefly address another approach that might be insightful when trying to solve such inverse problems. It is possible, either analytically or numerically, to calculate the temperature evolution through our sample as a function of time and space. This means, we approximately know the temperature at any given spot and time inside our sample. We also know, that any temperature is not equally as *possible*. Immediately after the system is spontaneously tilted out of its equilibrium state by the heat flux at t=0, it will start to increase its entropy. It does so, by annealing the temperature with its surrounding through convection and radiation; and within the body through conduction, since its state at t=0 is very unlikely and thus unstable. If we were to assume an adiabatic case, the entropy increase of our sample (which can be expressed as a function of probabilities) must be proportional to the added amount of heat - see Equation 2.3. As a consequence, we can obtain q and proceed to determine all of the above mentioned material properties. This approach relies on finding appropriate descriptors for the probability density functions, which may be modelled to the sub-atomic level or approximated with appropriate surrogates. Either way, we would need to establish a functional that takes the relative energy of a proportion of our sample (must be $\propto T^n$, could be the thermodynamic energy $k_b T$), as well the interaction between all proportions of our sample, into account. As we can see, this brings us close to the definitions of heat capacity. The deliberation of entropic approaches is nothing new, the whole field of statistical thermodynamics is based on it, and could be used as another layer to find suitable models for our material behavior during the laser flash experiment. Further investigations should be appropriately addressed in stand-alone work packages.

EXPERIMENTAL SCOPE, PRACTICAL IMPLEMENTATION

Any calculation, or other computational task, which was performed within the scope of this work, was implemented with the open source programming language Python (3.9.6).

4.1 TEMPERATURE MEASUREMENTS AND CALIBRATION

All experiments were conducted on a LFA 467 HyperFlash® from Netzsch Gerätebau GmbH (Selb, Germany). In order to calibrate it, we used a K-Type thermocouple (chromel/alumel, 1/0.3 mm diameter, specified to ANSI MC96.1 Class 1 tolerance) connected to a MCP9600 from Microchip Technology Inc. (Chandler, USA) on an evaluation board with the necessary driving circuit from MikroElektronika d.o.o. (Belgrad, Serbia). The thermocouple featured a miniature plug with connectors of the same metal as the respective wire, to enhance accuracy. The wires were isoloated with Teflon, the tip exposed and welded. An exposed tip is needed to ensure fast response times and accurate measurements by decreased influence of latent heat. Furthermore, the small diameter enabled guiding the wires through the cover of the apparatus, see Figure 14.
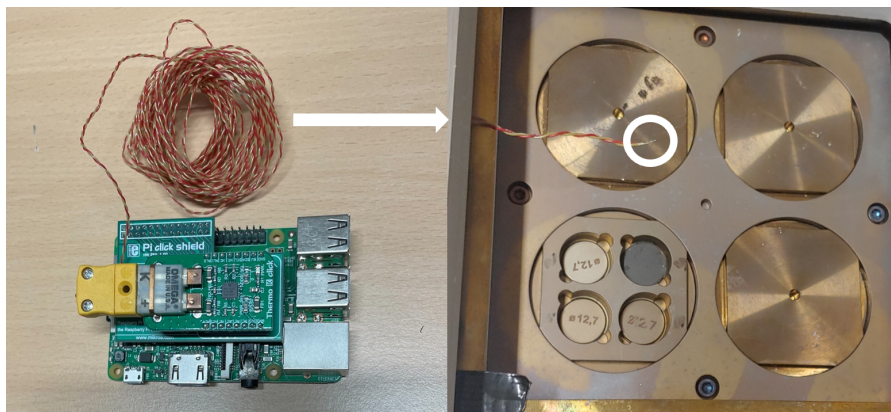
Figure 14: Thermocouple with Raspberry Pi (left) and exposed tip inside the machine (right)

The MCP9600 was accessed through a Raspberry Pi 3 B (as seen in Figure 14) via the I²C serial communication bus with a set bitrate of 50 kbps. The microchip includes hot-junction compensation (in form of a semiconductor temperature sensor), an 18-Bit analogue digital converter (ADC) and a math module that enables direct reading of temperature in °C or K. Appropriate scripts to automate the mea-

surements were written with the use of the *smbus* library. However, upon trying to verify the set-up, we noticed a significant mismatch between other calibrated temperature measurements. This either means, the *smbus* library is producing bogus values through bugs (interface problem), or the temperature sensor on the microchip is faulty. We couldn't verify either conjecture. The driver was adapted to directly read the register to which the ADC writes. As we knew the ADC resolution and the driving voltage, we could obtain the correct reading in mV. We used the ITS-90 reference function as specified in [75] to obtain the corresponding temperature, and corrected for the cold junction temperature by using calibrated room temperature measurements. The room climate was controlled and the measurement durations were short, therefore the influence of improper cold-junction compensation may be seen as neglectable. To validate the final set-up, we used a highly precise and homogeneous heating plate; as featured in an digital image correlation system - for the measurement of thermal expansion coefficients by Dantec Dynamics GmbH (Ulm, Germany). The plate is not only thermally controlled, but is also equipped with a calibrated temperature measurement system, which could be exploited to provide a baseline for our own thermal measurement set-up. The thermocouple was connected to the plate with a strip of adhesive polytetrafluorethylene (PTFE) tape, which also functioned as an insulator to reduce heat losses (note, the plate temperature is measured inside the plate near the surface). We could validate our driver, as shown in Figure 15.
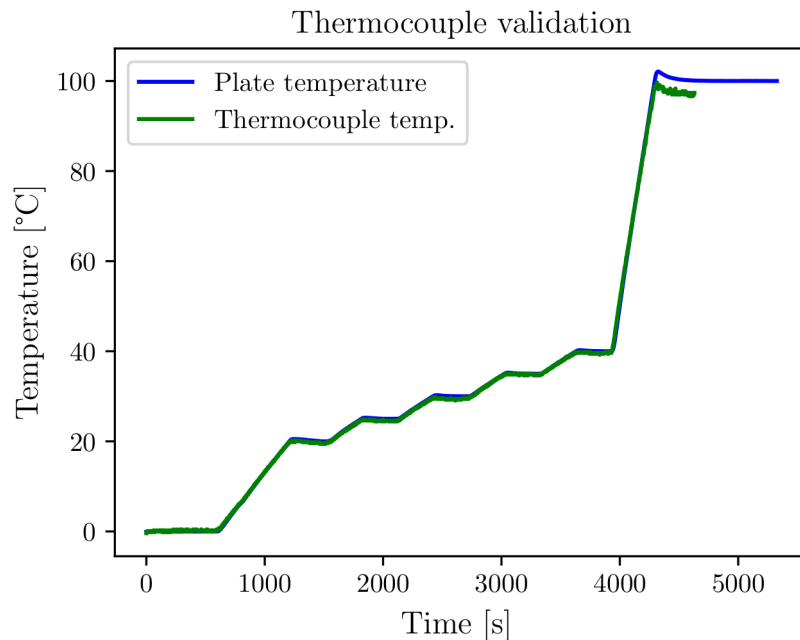

Figure 15: Validation of temperature sensor through heating plate

The calibration procedure of the mercury-cadmium-telluride IR-sensor inside the LFA 467 is then conducted as follows:

- Measure the temperature of a sample during an experiment inside machine with own sensor.

- Use a reference material of known thermophysical properties and calculate apparent heat flux for the corresponding laser setting (voltage of charging capacitor and pulse duration), repeat 3 times per setting.

- Measure the sample under same conditions with IR-sensor, correct for the now obtainable voltage drop curve of the flash lamp (the used LFA needs evaluable IR-sensor input to output data - which is not possible when the surface is obfuscated by the thermocouple), introduce a calibration factor to acquire temperature from voltage curve.

- Check if controllable or repeatable.

To optimize thermal contact between the sample and the thermocouple, silicon based thermal compound was used. The thermal compound had to be electrically insulating as the thermocouples would measure the electric potential of the conductor they are in contact with. Again, the thermocouple has been fixed with adhesive tape.

The temperature signal obtained through the thermocouples had to be manipulated to correctly evaluate it. This was done by applying a Butterworth filter (digital low-pass filter) to denoize it, and applying a Savitzky-Golay filter afterwards to smooth it, without loosing characteristic edges. We then calculated the first derivative of the smoothed curve, to obtain the starting point for the experiment (local minimum in front of the global maximum). This is needed, as we do not know the exact time the flash lamp activates when using the thermocouples. This enabled us to evaluate all measurements automatically. As an example, a temperature curve is depicted in Figure 16. Pyroceram was used as a reference material, the resulting ΔT and q_{app} are illustrated in Table 2

Table 2: Calibrating the apparatus through the measurement of pyroceram with thermocouple

Settings	ΔT [K]	q_{app} [J/cm²]
230 V & 1.5 ms	0.830 ± 0.44	0.445 ± 0.023
260 V & 1.0 ms	0.978 ± 0.40	0.524 ± 0.022
260 V & 1.5 ms	1.055 ± 0.31	0.555 ± 0.017

We then carried out three laser shots at the same sample at similar temperature, whilst using the IR-sensor, and used our obtained flash
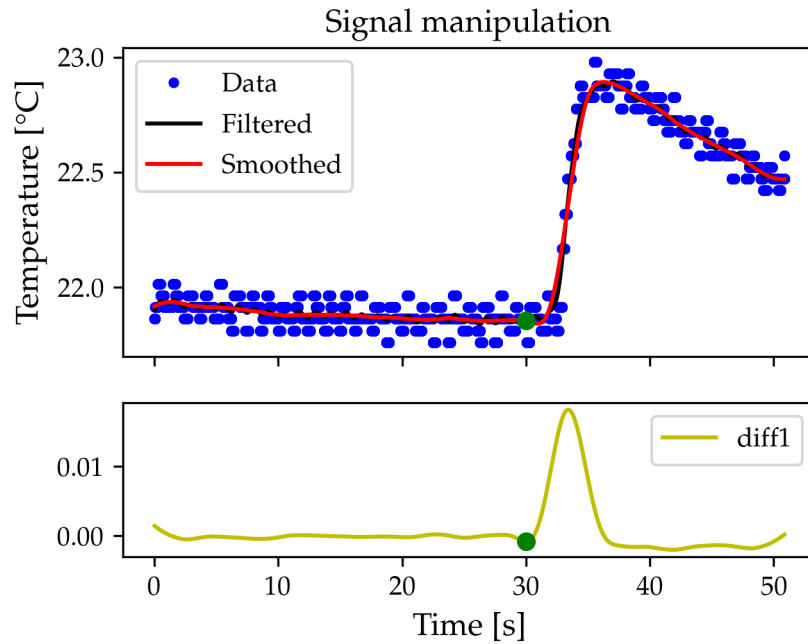
Figure 16: Example measurement of pyroceram with thermocouples

lamp characteristics to determine a calibration factor. To do so, we assumed the same shot settings will result in the same temperature rise. Dividing and averaging netted a factor of 0.10515 °C / V when using an amp gain of 10000x789. Thus, we found a definitve relationship between gain, voltage of the IR sensor and temperature to apply on other measurements. Furthermore, we found a correction factor for the heat flux energy by proceeding alike for the integral of the voltage drop at the flash lamp and the projected heat flux. We concluded the lamp delivers 0.147 J/cm² per unit "pulse integral" [Vms]. The last step was repeated a second time on another day (for the second round of samples, roughly a month apart) at elevated temperature (30 °C), with similar, yet not equal results. This might be due to the temperature difference or because of the lamp degrading and other general changes to the apparatus. Hence we can conclude, that a valid calibration would require us to repeat the total procedure (including the inconvenient thermocouple measurements), keep in mind that this was not done. The resulting temperature curves for pyroceram are illustrated in Figure 17.

4.2 MATERIALS AND SPECIMEN PRODUCTION

We used in total six materials, all of them commercially available, injection moulding grade thermoplastics. Three of them semi-crystalline (high-density polyethylene - HDPE, polybutylene therepthalate - PBT and a blend of PBT and polycarbonate PC - PBT/PC) and three amor-
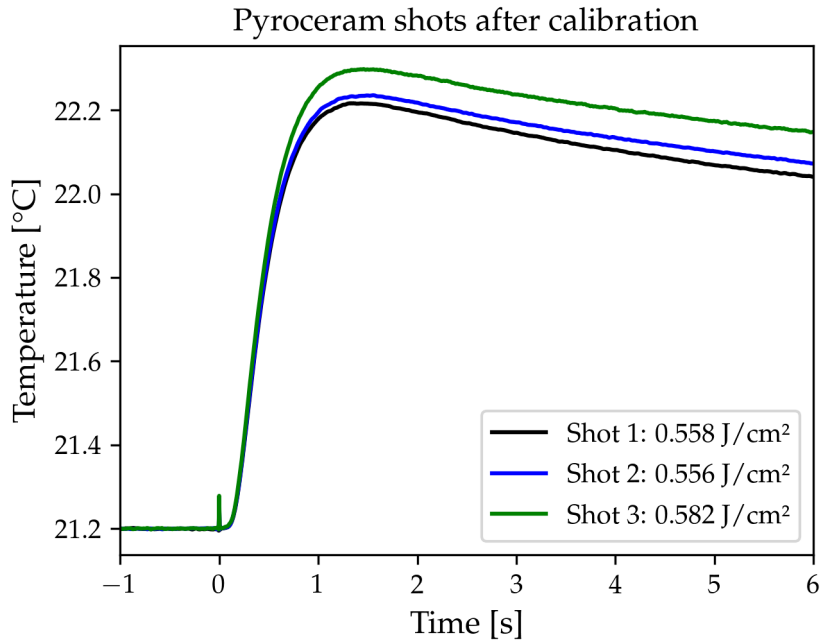
Figure 17: Shots at reference material (pyroceram), recorded with IR-sensor after calibration

phous (acrylonitrile butadiene styrene - ABS, polymethyl methacrylate - PMMA and PC). They were acquired in the form of pellets. The LFA - as well as the GHFM measurements, required flat cylindrical samples. Ideally, LFA measurements of thermal insulators are conducted on thin samples, however, GHFM measurements should use thicker samples. As the focus is on LFA measurements, we decided to press roughly 1 mm thick plates to then obtain both our samples. We did not choose to manufacture plates of different thickness, because processing is a crucial factor influencing the properties of polymers, and should be minimized as much as possible when testing for physical properties. Most of our samples, with the exception of HDPE, were sensible to moisture (polyesters and/or polar polymers), therefore all of them have been air dried according to the suggestion of the respective producer (minimum time, not exceeding it more than four hours). Directly after drying we transferred the warm pellets to a Collin P 200 T hydraulic platen press from COLLIN Lab & Pilot Solutions GmbH (Maitenbeth, Germany), using cut-out metal sheets to form 160 x 160 x 1 mm plates. This machine is able to run a 3 step program (set hydraulic pressure up to 6.5 bar, temperature up to 300 °C and step duration). To find optimal settings we conducted a quick parameter study to find general influences on the respective material, which we then evaluated optically for defects (air inclusions, weld or flow lines, burn marks, discolouration, etc.) and ultimately optimized the parameters by trial and error. We had to use a silicon based demoulding agent for PC and PBT/PC. The final settings which yielded

plates of acceptable, visually determined, quality are displayed in Table 3.

Table 3: Parameters used to manufacture plates for specimen production

Material	ABS			HDPE		
Step	1	2	3	1	2	3
Pressure [bar]	1	6.5	6.5	1	6.5	6.5
Temperature [°C]	200	180	30	180	180	30
Time [s]	300	300	330	600	600	300
Material	PBT, PBT/PC			PC, PMMA		
Step	1	2	3	1	2	3
Pressure [bar]	1	6.5	6.5	1	6.5	6.5
Temperature [°C]	230	225	30	250	240	30
Time [s]	300	300	330	500	300	360

The specimen for LFA measurements were punched out of the plates, using a hollow punch with a diameter of 12.6 mm and a hammer. For the guarded heat flow meter, the samples needed to be circular with a diameter of 50 mm, which required using a hand actuated hydraulic press to do punch/cut (mechanism depending the brittleness, due to slow impact) to according size. DSC samples have been extracted using a scalpel, it was tried to match the weight of the reference material (sapphire crystal) at 32.68 mg. Specimen for density measurements were cut with a knife and it was ensured that their weight is above 1 g to enhance accuracy.

After processing, all plates have been kept in a room with standardized climate (DIN EN ISO 291 class 2), for at least one day and at most four weeks, until sample collection. LFA and GHFM specimen were stored inside sealed plastic bags. DSC and density specimen were tested immediately upon cutting.

As discussed, LFA specimen need special graphite coating to match necessary optical boundary conditions. This is achieved through the application of dissolved graphite flakes (with "graphite sprays"). During this work, it was discovered that the graphite spray, *which is recommended by the LFA OEM for plastics*, contains acetone. Unfortunately, acetone is a potent solvent for many thermoplastics - especially for the used ABS. This was unravelled because the samples were rechecked after the first round of LFA tests. As expectable, we could immediatly notice surface changes in the ABS specimen ("tacky" feeling when touched, graphite "coating" not removable as flakes diffused inside the material). For the second round we used a different, acetone-free spray for coating. Please note, that we will still provide the results

to discuss the influence of poor sample preparation. Henceforth, the measurements affected will be highlighted in red.

4.3 TECHNICAL DETAILS AND MEASUREMENT PARAMETERS

The evaluation methods have been disclosed in Section 2.6, the procedure for LFA measurements has been discussed in-depth throughout the last sections. For thermal diffusivity calculation we used the "Standard" model inside software package of the OEM (descriptively mentioned in Section 3.3). Each sample is measured three times at ≈ 30 °C, the diffusivity is calculated for each shot and then averaged over all shots. Within the individual shots we can expect good repeatability, with standard deviations of 1 % and lower, if, but only if, the evaluation method is applicable. This was the case for most measurements, except for the ABS sample that came in contact with acetone.

The densities are obtained at room temperature (22 °C) with a laboratory balance and an appropriate density measuring kit of Mettler Toledo (Greifensee, Switzerland). Each material was measured three times.

GHFM measurements were carried out using a DTC-300 from TA Instruments (New Castle, USA). The measurement is controlled as to achieve a medium temperature that is set beforehand to 30 °C (gradient method, thus $\lambda(T) \approx \lambda(T_{medium})$). Each material was measured three times, the thickness of each sample was measured at five points with a digital calliper. Thermal compound was used to optimize the thermal contact between the plates and the samples.

DSC measurements were performed on a Perkin Elmer Heat Flux DSC 4000 (PerkinElmer Inc., Waltham, Massachusetts, USA) with a heating rate of 10 K/min, the heating curves were evaluated continuously from -10 °C to 45 °C. The thermal history of the material was not eliminated, as is the case with other experiments. Ultimately, the heat capacity is obtained at 30 °C, again, for three different samples per material.

RESULTS AND DISCUSSION

Starting this chapter we will foremost address the acetone spray issue by comparing the thermal diffusivities of all samples as seen in Table 4, affected samples marked red.

Table 4: Measured thermal diffusivities, evaluated with OEM software (adapted Cape-Lehmann model [11])

	Thermal diffusivity [mm²/s]			Standard deviation [%]		
Sample No.	1	2	3	1	2	3
ABS	0.144	0.116	0.118	4.62	0.50	0.49
HDPE	0.257	0.282	0.277	0.67	0.20	1.46
PMMA	0.128	0.117	0.113	0.78	1.40	0.51
PBT	0.142	0.142	0.149	0.40	0.40	0.00
PBT/PC	0.136	0.134	0.131	0.42	0.86	0.44
PC	0.157	0.15	0.151	0.37	0.00	0.38

The ABS sample, which was coated with the acetone-containing graphite spray, did not only show a significantly higher (>20%) thermal diffusivity in comparison, but also higher variation when using the "Standard" evaluation method. Likewise, PMMA also exhibits an increase, but falls short with >9% difference. Because the calculation of thermal diffusivity is directly dependent on the square of the measured thickness, we could conjecture, that if the sample swells after the fact, we unknowingly increase the thickness and underestimate diffusivity. This seems to not be the most probable case for ABS. Likely, we will also alter the optical properties of our substance since the graphite diffuses inside the substance and may not be seen as a layer on top, but rather acts like a filler near the outer ends of our body. This can be made evident when looking at the temperature rise curves, as not fully opaque specimen typically produce an "irridiation peak", as seen in Figure 18. Followed by an immediate temperature increase throughout the substance, before we are able to observe the characteristic temperature rise at the rear surface. This could be mitigated by using available models that consider such mechanisms. Additionally, there is a chance that we also physically altered thermodynamic properties. However, since the amount of the solvent is miniscule in comparison to the mass of our sample - we are uncertain to which degree this would come to effect. To provide definitive statements, this would need to be subjected to further research.

Ideally, we should strive to eliminate the need for coatings, by incorporating optical properties and regard them appropriately in our evaluation models. More so, because we see an adversary coating effect in HDPE, with a >9% lower diffusivity of the sample which was subjected to acetone, meaning we can not see unambiguous effects. Figure 19 shows this exactly different behavior. Another possible explanation would be, that the two sprays lead to drastically different optical boundaries - such that translucent/colorless samples (ABS, HDPE and PMMA; PBT, PC, PBT/PC were all black) are affected more so.
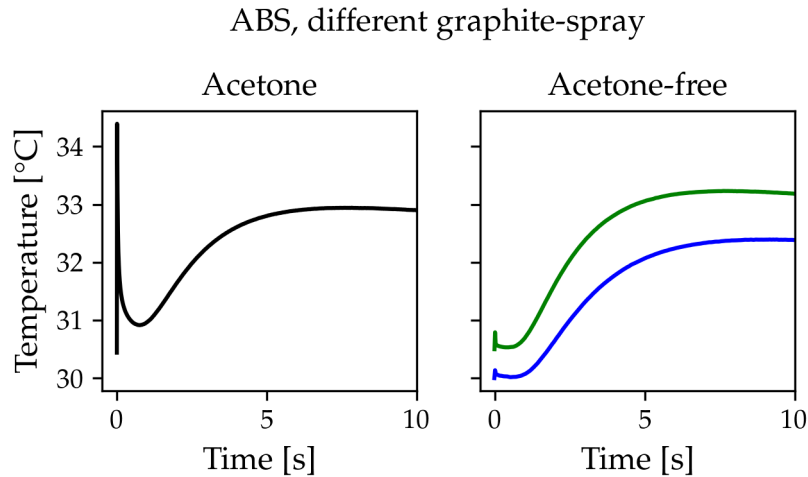

Figure 18: The influence of graphite-coating containing acetone on three different samples
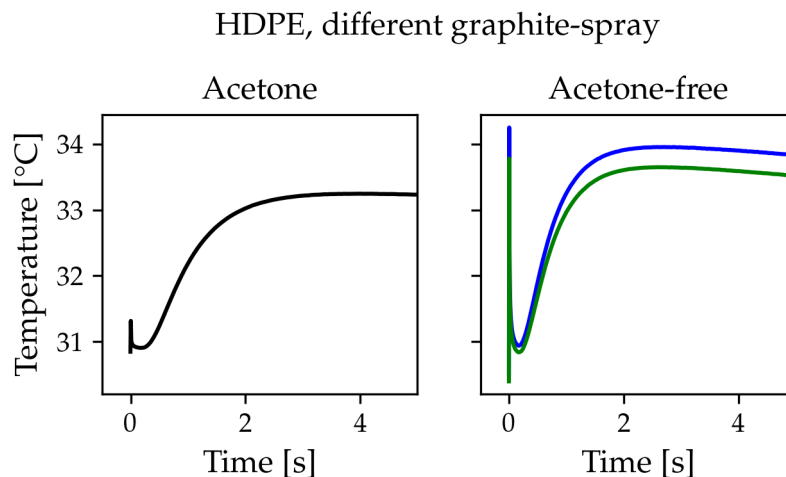

Figure 19: The influence of graphite-coating containing acetone on three different samples

Since the volumetric heat capacity k is formed by multiplication of two measured values we need to account for error propagation to de-

fine the uncertainty. We will write the error as Δ_k. To quantify errors we will use the standard deviation of the mean for each variable Δ_λ and Δ_ρ and state:

$$k + \Delta_k = (\lambda \Delta_\lambda)(\rho + \Delta_\rho)$$

Upon multiplying we will disregard $\Delta_\rho \Delta_\lambda$, since it's very small in comparison to the other terms, and write the total error as:

$$\Delta_k = \lambda \Delta_\rho + \rho \Delta_\lambda \tag{5.1}$$

In regards to the error calculation for our LFA methods - we will not treat every single shot at a sample as a different experiment like we did above. We obtain the standard deviation by the deviations of the calculated properties for each material. By implication, we consider three shots at one sample as the measurement result itself. Again, we will provide the incorrectly coated samples marked in red separately. Keep in mind, the uncertainty of LFA measurements is therefore composed by only two data points (of correctly coated samples) and needs to be subject of further scrutiny.

Table 5: Measurement results and comparison with instrumented results obtained via LFA

Property	PMMA	HDPE	ABS
ρ [g/cm³]	1.184 ± 0.0008	0.9483 ± 0.008	1.0407 ± 0.0005
c_p [J/gK]	1.45 ± 0.06	1.88 ± 0.05	1.37 ± 0.05
k [J/cm³K]	1.71 ± 0.07	1.78 ± 0.06	1.42 ± 0.05
$k_{1,LFA}$ [J/cm³K]	1.68	1.77	1.51
$k_{1,LFA}$ [J/cm³K]	1.63 ± 0.14	1.43 ± 0.09	1.61 ± 0.14
λ [W/mK]	0.204 ± 0.002	0.416 ± 0.006	0.164 ± 0.001
$\lambda_{1,LFA}$ [W/mK]	0.218	0.454	0.218
$\lambda_{1,LFA}$ [W/mK]	0.233 ± 0.058	0.400 ± 0.024	0.238 ± 0.060
Property	PBT	PBTPC	PC
ρ [g/cm³]	1.314 ± 0.005	1.3117 ± 0.0031	1.1897 ± 0.0047
c_p [J/gK]	1.28 ± 0.07	1.21 ± 0.06	1.26 ± 0.02
k [J/cm³K]	1.68 ± 0.09	1.59 ± 0.08	1.50 ± 0.03
$k_{1,LFA}$ [J/cm³K]	1.75	1.66	1.54
$k_{1,LFA}$ [J/cm³K]	1.64 ± 0.15	1.66 ± 0.13	1.64 ± 0.13
λ [W/mK]	0.249 ± 0.006	0.215 ± 0.004	0.215 ± 0.007
$\lambda_{1,LFA}$ [W/mK]	0.248	0,226	0.241
$\lambda_{1,LFA}$ [W/mK]	0.278 ± 0.075	0.264 ± 0.067	0.250 ± 0.057

Table 5 shows the measured densities (hydrostatic weighing), specific heat capacities under constant pressure (DSC) and thermal conductivities (GHFM), including their standard deviations; as well as

the calculated volumetric heat capacity with the emerging measurement uncertainty. Furthermore, Table 5 compares the calculated values from LFA measurements for the corresponding property - which we obtained by calibrating the machine and using a reference measurement for heat flux determination, to achieve proper instrumentation. Values which were derived with our calibration approach are marked with the subscript 1 ($k_{1,LFA}$ & $\lambda_{1,LFA}$).

The respective ΔT and q_0, which emerged from our measurements are illustrated in Table 6, and seem to be in a physically reasonable range for our samples with $L \approx 1mm$.

Table 6: Resulting ΔT and q_{corr} from our instrumented measurements for sanity-check

	ΔT [K]			q_{corr}[J/cm²]		
Sample No.	1	2	3	1	2	3
ABS	2.93	2.41	2.56	0.565	0.573	0.575
HDPE	2.41	2.86	2.98	0.559	0.569	0.568
PMMA	2.94	2.78	2.76	0.566	0.565	0.565
PBT	2.71	3.21	3.11	0.566	0.570	0.569
PBT/PC	2.75	2.95	2.85	0.569	0.567	0.567
PC	2.81	2.81	2.79	0.569	0.566	0.566

As it can be seen in Table 5, the results of the first round of instrumented shots, are - despite the coating issue - within margin of error for k. This can be seen as a success. The accuracy of the second round of the instrumented shots is decreased - most likely because we did not repeat the full calibration procedure for the IR sensor during the second round. Coincidentally the flash lamp also neared its end of life at the time. Meaning, we likely overestimated q_0. λ strongly depends on the evaluation method for the diffusivity. The various available methods are based on different physical concepts, which need to be able to correctly map our experiment. For reference, the best methods (included in the software of the OEM) would yield great improvements for $\lambda_{1,LFA}$ in W/mK: HDPE (model: "Penetration") 0.408 vs. 0.416, PBT (model: "Adiabatic"): 0.256 vs. 0.249, PBTPC (model: "Penetration") 0.214 vs. 0.215, PC (model: "Penetration") 0.223 vs. 0.215, ABS (model: "Adiabatic") 0.15 vs 0.164 and PMMA (model: "Transparent") 0.205 vs. 204. As almost all of the best fitting models (except PBT) regard optical properties, we can conclude, that this is in fact a crucial point when testing polymers with the laser flash method. The accuracy of the ABS fits obviously suffer from poor sample prepara-

tion.

Table 7 compares the results of our inverse engineered shots to the corresponding measured properties, which are obtainable if *only* the temperature response is known. As we encountered some problems with the data output of the raw voltage signal from the IR-sensor (and the automated computing on our side), we used just one shot at each sample to inversely fit the material properties. This evaluation method is marked with the subscript 2.

Table 7: Measurement results and comparison with inverse engineered results obtained via LFA

Property	PMMA	HDPE	ABS
k [J/cm³K]	1.71 ± 0.07	1.78 ± 0.06	1.42 ± 0.05
$k_{2,LFA}$ [J/cm³K]	2.09	1.53	1.20
$k_{2,LFA}$ [J/cm³K]	1.64 ± 0.33	1.64 ± 0.00	1.20 ± 0.00
λ [W/mK]	0.204 ± 0.002	0.416 ± 0.006	0.164 ± 0.001
$λ_{2,LFA}$ [W/mK]	0,284	0,423	0,182
$λ_{2,LFA}$ [W/mK]	0.262 ± 0.017	0.402 ± 0.062	0.163 ± 0.001
Property	PBT	PBTPC	PC
k [J/cm³K]	1.68 ± 0.09	1.59 ± 0.08	1.50 ± 0.03
$k_{2,LFA}$ [J/cm³K]	1.87	1.64	1.31
$k_{2,LFA}$ [J/cm³K]	1.53 ± 0.11	1.2 ± 0.00	1.2 ± 0.00
λ [W/mK]	0.249 ± 0.006	0.215 ± 0.004	0.215 ± 0.007
$λ_{2,LFA}$ [W/mK]	0.286	0.247	0.227
$λ_{2,LFA}$ [W/mK]	0.240 ± 0.020	0.182 ± 0.002	0.199 ± 0.001

The calculated values we obtained by inversely fitting the measurement in Table 7 show, that we ran into our lower boundaries for k for PBTPC, PC and ABS in the second round; and for ABS in the first round. Not because the range is too limited, but the model fails to correctly represent these shots, because it underestimates the heat loss due to our approximations. Obviously, we still rely on the input of a thermal diffusivity for this procedure - we have used the "Standard" method as above. Those steps could be automated further, as the quality of a fit, which is constrained by a true physical model, can be quantified by any measure for deviation to experimental curve, such as mean square error. This could be even more fruitful than the improved instrumentation for the determination of λ, as suggested by Table 8 - which finally compares the accuracy of both approaches to one another. As it can be seen, while we may overestimated q_0 through $ΔT_{max}$ and a through the "Standard" model, $λ_{2,LFA}$ tends to

give the closest approximate in the second round - as the model maximizes the heat loss effect through lowering k. Which accordingly results in a reduced λ. The overestimation of ΔT_{max} might be corrected by including optical properties of our substance.

Table 8: Overview of the precision of both proposed methods

Deviation to expected value [%]			
Intrumented			
Material	$k_{1,LFA}$	$k_{1,LFA}$	$\lambda_{1,LFA}$	$\lambda_{1,LFA}$
PMMA	-2.15	-5.09	6.81	14.35
HDPE	-0.95	-19.98	9.31	-3.65
ABS	6.38	13.32	32.68	45.22
PBT	3.81	-2.46	-0.34	11.86
PBTPC	4.55	4.32	5.31	22.9
PC	2.26	9.02	11.94	16.11
Average Deviation (abs)	3.35	9.03	11.07	19.01
Inverse engineered			
Material	$k_{2,LFA}$	$k_{2,LFA}$	$\lambda_{2,LFA}$	$\lambda_{2,LFA}$
PMMA	21.98	-3.97	39.44	28.76
HDPE	-14.09	-7.86	1.82	-3.40
ABS	-15.52	-15.52	11.22	-0.49
PBT	11.04	-8.79	14.85	-3.43
PBTPC	3.27	-24.64	14.73	-15.44
PC	-12.67	-20.07	5.34	-7.77
Average Deviation (abs)	13.10	13.48	14.57	9.88

Lastly, we need to add, that some of the error for PBTPC - which showed elevated divergence despite not being translucent - may be referred back to difficulties in processing such a blend, as we are severely limited by the homogenization capabilities of the press. Due to viscosity differences in the two materials, they are prone to separate by flowing at different speeds inside the press. And as the LFA samples are small, we are more likely to retrieve samples with severe differences in their constitution.

CONCLUDING REMARKS

We have managed to establish two approaches, that permit us to calculate all relevant thermophysical properties of polymers - with just one single transient, opto-thermal measurement. The first method proposed aimed at improving the technical set-up of commonly used LFA testing devices, through true physical measurements. We included suggestions and concepts for implementation. The second method framed the measurement as an inverse problem, in order to acquire additional information from the generated dataset - which would be hidden for legacy evaluation methods.

Both procedures were evaluated in their eligibility by an experimental series conducted on six different polymers. The accuracy was found to be reasonable for a proof of concept, but may be improved greatly by improving our simple model and makeshift instrumentation. The crucial elements in which the modelling/instrumentation would need to be improved have been presented and discussed.

Additionally, we provided thoughts and concepts, which might be able to contribute to the solution of the proposed problem, within the domain of statistical thermodynamics.

Furthermore, we found experimental proof, that the common practice of coating samples with graphite spray should always be questioned, and at best, omitted. If it is necessary - it might be beneficial to regard it within the evaluation (i.e. using a multi-layered model).

[1]   URL: https://www.webofscience.com/.

[2]   C. Arthur. *Tech giants may be huge, but nothing matches big data.* Ed. by T. Guardian. 2013. URL: https://www.theguardian.com/technology/2013/aug/23/tech-giants-data.

[3]   Atkins and P. W. "Laws of Thermodynamics: A Very SHort Introduction." In: (2010).

[4]   T. Azumi and Y. Takahashi. "Novel finite pulse–width correction in flash thermal diffusivity measurement." In: *Review of Scientific Instruments* 52.9 (1981), pp. 1411–1413. ISSN: 0034-6748. DOI: 10.1063/1.1136793.

[5]   S. G. Balogh, G. Palla, P. Pollner, and D. Czégel. "Generalized entropies, density of states, and non-extensivity." In: *Scientific reports* 10.1 (2020), pp. 1–12.

[6]   J. V. Beck. "Transient determination of thermal properties." In: *Nuclear Engineering and Design* 3.3 (1966), pp. 373–381. ISSN: 0029-5493. DOI: 10.1016/0029-5493(66)90128-2.

[7]   J. V. Beck. *The optimum analytical design of transient experiments for simultaneous determinations of thermal conductivity and specific heat.* Michigan State University, 1964.

[8]   A. Bejan and A. D. Kraus. *Heat transfer handbook.* New York: J. Wiley, 2003. ISBN: 0471390151.

[9]   D. Bernoulli. *Hydrodynamica: sive de viribus et motibus fluidorum commentarii.* 1738.

[10]   R. Bhowmik, S. Sihn, V. Varshney, A. K. Roy, and J. P. Vernon. "Calculation of specific heat of polymers using molecular dynamics simulations." In: *Polymer* 167 (2019), pp. 176–181. ISSN: 00323861. DOI: 10.1016/j.polymer.2019.02.013.

[11]   J. Blumm and J. Opfermann. "Improvement of the mathematical modeling of flash measurements." In: *High Temperatures-High Pressures* 34.5 (2002), pp. 515–521. ISSN: 0018-1544. DOI: 10.1068/htjr061.

[12]   L. Boltzmann. *Über die mechanische Bedeutung des zweiten Hauptsatzes der Wärmetheorie:(vorgelegt in der Sitzung am 8. Februar 1866).* Staatsdruckerei, 1866.

[13]   E. Callaway. "'It will change everything': DeepMind's AI makes gigantic leap in solving protein structures." In: *Nature* 588.7837 (2020), pp. 203–204. ISSN: 1476-4687. DOI: 10.1038/d41586-020-03348-4.

[14]   J. A. Cape and G. W. Lehman. "Temperature and Finite Pulse–Time Effects in the Flash Method for Measuring Thermal Diffusivity." In: *Journal of Applied Physics* 34.7 (1963), pp. 1909–1913. ISSN: 0021-8979. DOI: 10.1063/1.1729711.

[15]   H. S. Carslaw and J. C. Jaeger. *Conduction of heat in solids*. 2. ed., reprinted. Oxford science publications. Oxford: Clarendon Press, 2008. ISBN: 0198533683.

[16]   Y. A. Cengel, M. A. Boles, and M. Kanoglu. *Thermodynamics: an engineering approach*. Vol. 5. McGraw-hill New York, 2011.

[17]   F. C. Chen, Y. M. Poon, and C. L. Choy. "Thermal diffusivity of polymers by the flash method." In: *Polymer* 18.2 (1977), pp. 129–136. ISSN: 00323861. DOI: 10.1016/0032-3861(77)90027-1. URL: https://www.sciencedirect.com/science/article/pii/0032386177900271.

[18]   S. Z. Cheng. *Handbook of Thermal Analysis and Calorimetry: Applications to Polymers and Plastics*. Elsevier, 2002. ISBN: 0444512861.

[19]   Y. Chihab, M. Garoum, and N. Laaroussi. "A New Efficient Formula for the Thermal Diffusivity Estimation from the Flash Method Taking into Account Heat Losses in Rear and Front Faces." In: *International Journal of Thermophysics* 41.8 (2020). ISSN: 1572-9567. DOI: 10.1007/s10765-020-02704-w.

[20]   C.-P. Chiu, J. G. Maveety, and Q. A. Tran. "Characterization of solder interfaces using laser flash metrology." In: *Microelectronics Reliability* 42.1 (2002), pp. 93–100. ISSN: 00262714. DOI: 10.1016/S0026-2714(01)00129-9.

[21]   C. L. Choy. "Thermal conductivity of polymers." In: *Polymer* 18.10 (1977), pp. 984–1004. ISSN: 00323861. DOI: 10.1016/0032-3861(77)90002-7.

[22]   L. M. Clark III and R. E. Taylor. "Radiation loss in the flash method for thermal diffusivity." In: *Journal of Applied Physics* 46.2 (1975), pp. 714–719. ISSN: 0021-8979. DOI: 10.1063/1.321635.

[23]   R. Clausius. "Ueber die bewegende Kraft der Wärme und die Gesetze, welche sich daraus für die Wärmelehre selbst ableiten lassen." In: *Annalen der Physik* 155.3 (1850), pp. 368–397. ISSN: 0003-3804.

[24]   R. Clausius. "The Mechanical Theory of Heat." In: (1879).

[25]   M. J. Colaço, H. R. B. Orlande, and G. S. Dulikravich. "Inverse and optimization problems in heat transfer." In: *Journal of the Brazilian Society of Mechanical Sciences and Engineering* 28.1 (2006), pp. 1–24. ISSN: 1678-5878. DOI: https://doi.org/fht66g.

[26]   R. D. Cowan. "Pulse Method of Measuring Thermal Diffusivity at High Temperatures." In: *Journal of Applied Physics* 34.4 (1963), pp. 926–927. ISSN: 0021-8979. DOI: 10.1063/1.1729564.

[27] P. Debye. "Zur Theorie der spezifischen Wärmen." In: *Annalen der Physik* 344.14 (1912), pp. 789–839. ISSN: 0003-3804. DOI: 10.1002/andp.19123441404.

[28] S. Dong, A. Sheldon, and K. Carney, eds. *Modeling of Carbon-Fiber-Reinforced Polymer (CFRP) Composites in LS-DYNA with Optimization of Material and Failure Parameters in LS-OPT*. 2018.

[29] P. L. Dulong and A.-T. Petit. *Recherches sur quelques points importans de la theorie de la chaleur*. 1819.

[30] G. W. Ehrenstein, G. Riedel, and P. Trawiel. *Thermal Analysis of Plastics: Theory and Practice*. Carl Hanser Verlag GmbH Co KG, 2012. ISBN: 9783446434141.

[31] A. Einstein. *Planck's theory of radiation and the theory of specific heat*. 1907. URL: https://scholar.google.com/citations?user=qc6cjjyaaaaj&hl=en&oi=sra.

[32] Y. Escoufier. "Preface of Data Science and Its Applications." In: (1995).

[33] D. J. Evans, S. R. Williams, and D. J. Searles. "A proof of Clausius' theorem for time reversible deterministic microscopic dynamics." In: *The Journal of chemical physics* 134.20 (2011), p. 204113. ISSN: 0021-9606.

[34] R. Feistel. "Distinguishing between Clausius, Boltzmann and Pauling entropies of frozen non-equilibrium states." In: *Entropy* 21.8 (2019), p. 799.

[35] L. Finegold and S. E. Moody. "Debye and Tarasov Specific Heat Models: Solution of Integral Equation." In: *American Journal of Physics* 40.6 (1972), pp. 915–916. ISSN: 0002-9505. DOI: 10.1119/1.1986698.

[36] J. B. J. b. Fourier. *The Analytical Theory of Heat*. The University Press, 1878.

[37] U. Gaur and B. Wunderlich. "Heat Capacity and Other Thermodynamic Properties of Linear Macromolecules. V. Polystyrene." In: *Journal of Physical and Chemical Reference Data* 11.2 (1982), pp. 313–325. ISSN: 0047-2689. DOI: 10.1063/1.555663.

[38] B. Gebhart, Y. Jaluria, R. L. Mahajan, and B. Sammakia. *Buoyancy-induced flows and transport*. United States: Hemisphere Publishing, New York USA, 1988. URL: https://www.osti.gov/biblio/6546182.

[39] Y. K. Godovsky. *Thermophysical Properties of Polymers*. Springer Science & Business Media, 2012. ISBN: 9783642516702.

[40] G. X. Gu, C.-T. Chen, D. J. Richmond, and M. J. Buehler. "Bioinspired hierarchical composite design using machine learning: simulation, additive manufacturing, and experiment." In: *Materials Horizons* 5.5 (2018), pp. 939–945. ISSN: 2051-6347. DOI: 10.1039/C8MH00653A.

[41] E. A. Guggenheim. "Thermodynamics-an advanced treatment for chemists and physicists." In: *Amsterdam* (1985).

[42] D. M. Hawkins. "The problem of overfitting." In: *Journal of Chemical Information and Computer Sciences* 44.1 (2004), pp. 1–12. ISSN: 0095-2338. DOI: 10.1021/ci0342472.

[43] W. Hu. "The physics of polymer chain-folding." In: *Physics Reports* 747 (2018), pp. 1–50. ISSN: 0370-1573. DOI: 10.1016/j.physrep.2018.04.004. URL: https://www.sciencedirect.com/science/article/pii/S0370157318301042.

[44] IDC. *Revenue from big data and business analytics worldwide from 2015 to 2022 (in billion U.S. dollars)*. Ed. by Statista. URL: https://www.statista.com/statistics/551501/worldwide-big-data-business-analytics-revenue/.

[45] F. P. Incropera. *Fundamentals of heat and mass transfer*. 6th ed. Hoboken NJ: John Wiley, 2007. ISBN: 0471457280.

[46] R. Jakobi, E. Gmelin, and K. Ripka. "High-precision adiabatic calorimetry and the specific heat of cyclopentane at low temperature." In: *Journal of Thermal Analysis* 40.3 (1993), pp. 871–876. ISSN: 0368-4466. DOI: 10.1007/BF02546845.

[47] E. T. Jaynes. "Gibbs vs Boltzmann Entropies." In: *American Journal of Physics* 33.5 (1965), pp. 391–398. ISSN: 0002-9505. DOI: 10.1119/1.1971557.

[48] J. P. Joule. "V. On some thermo-dynamic properties of solids." In: *Philosophical Transactions of the Royal Society of London* 149 (1859), pp. 91–131. ISSN: 0261-0523. DOI: 10.1098/rstl.1859.0005.

[49] D. Kern GmbH Großmaischeid, ed. URL: https://www.kern.de/de/richtwerttabelle.

[50] R. C. Kerschbaumer et al. "Comparison of steady-state and transient thermal conductivity testing methods using different industrial rubber compounds." In: *Polymer Testing* 80 (2019), p. 106121. ISSN: 01429418. DOI: 10.1016/j.polymertesting.2019.106121.

[51] A. Kiessling, D. N. Simavilla, G. G. Vogiatzis, and D. C. Venerus. "Thermal conductivity of amorphous polymers and its dependence on molecular weight." In: *Polymer* 228 (2021), p. 123881. ISSN: 00323861. DOI: 10.1016/j.polymer.2021.123881.

[52]   B. Kozanoglu and J. Lopez. "Thermal boundary layer and the characteristic length on natural convection over a horizontal plate." In: *Heat and mass transfer* 43.4 (2007), pp. 333–339.

[53]   B. Lin, S. Zhu, H. Ban, C. Li, R. N. Scripa, C.-H. Su, and S. L. Lehoczky. "Modified Laser Flash Method for Thermal Property Measurements and the Influence of Heat Convection." In: *Heat Transfer, Volume 1*. ASMEDC, 11152003, pp. 163–169. ISBN: 0-7918-3718-1. DOI: 10.1115/IMECE2003-41734.

[54]   D. Liu and C. Zhong. "Modeling of the Heat Capacity of Polymers with the Variable Connectivity Index." In: *Polymer Journal* 34.12 (2002), pp. 954–961. ISSN: 1349-0540. DOI: 10.1295/polymj. 34.954. URL: https://www.nature.com/articles/pj2002139.

[55]   A. Luikov. *Analytical Heat Diffusion Theory*. Elsevier, 1968. ISBN: 9780124597563. DOI: 10.1016/B978-0-12-459756-3.X5001-9.

[56]   A. Lunev, V. Zborovskii, and T. Aliev. "Complexity matters: Highly-accurate numerical models of coupled radiative–conductive heat transfer in a laser flash experiment." In: *International Journal of Thermal Sciences* 160 (2021), p. 106695. ISSN: 12900729. DOI: 10.1016/j.ijthermalsci.2020.106695.

[57]   L. Masanes and J. Oppenheim. "A general derivation and quantification of the third law of thermodynamics." In: *Nature communications* 8 (2017), p. 14538. DOI: 10.1038/ncomms14538.

[58]   J. C. Maxwell. "Illustrations of the dynamical theory of gases. Part II. On the process of diffusion of two or more kinds of moving particles among one another." In: *The London, Edinburgh, and Dublin Philosophical Magazine and Journal of Science* 20.130 (1860), pp. 21–37. ISSN: 1941-5982.

[59]   R. L. McMasters, J. V. Beck, R. B. Dinwiddie, and H. Wang. "Accounting for Penetration of Laser Heating in Flash Thermal Diffusivity Experiments." In: *Journal of Heat Transfer* 121.1 (1999), pp. 15–21. ISSN: 0022-1481. DOI: 10.1115/1.2825929.

[60]   H. Mehling, G. Hautzinger, O. Nilsson, J. Fricke, R. Hofmann, and O. Hahn. "Thermal Diffusivity of Semitransparent Materials Determined by the Laser-Flash Method Applying a New Analytical Model." In: *International Journal of Thermophysics* 19.3 (1998), pp. 941–949. ISSN: 1572-9567. DOI: https://doi.org/ d4h65t. URL: https://link.springer.com/article/10.1023/a: 1022611527321.

[61]   N. Mehra, L. Mu, T. Ji, X. Yang, J. Kong, J. Gu, and J. Zhu. "Thermal transport in polymeric materials and across composite interfaces." In: *Applied Materials Today* 12 (2018), pp. 92–130. ISSN: 23529407. DOI: 10.1016/j.apmt.2018.04.004.

[62] N. Milosevic, M. Raynaud, and K. Maglic. "Estimation of thermal Contact Resistance Between the Materials of Double-Layer Sample Using the Laser Flash Method." In: *Inverse Problems in Engineering* 10.1 (2002), pp. 85–103. DOI: `https://doi.org/bt4d9s`.

[63] A. Mirhoseini et al. "A graph placement methodology for fast chip design." In: *Nature* 594.7862 (2021), pp. 207–212. ISSN: 1476-4687. DOI: `10.1038/s41586-021-03544-w`.

[64] W. J. Parker, R. J. Jenkins, C. P. Butler, and G. L. Abbott. "Flash Method of Determining Thermal Diffusivity, Heat Capacity, and Thermal Conductivity." In: *Journal of Applied Physics* 32.9 (1961), pp. 1679–1684. ISSN: 0021-8979. DOI: `10.1063/1.1728417`.

[65] M. Planck. "Transcript of "Vorlesungen ueber Thermodynamik": Project Gutenberg EBook #31564." In: (2010).

[66] M. Polanco-Loria, H. Daiyan, and F. Grytten. "Material parameters identification: An inverse modeling methodology applicable for thermoplastic materials." In: *Polymer Engineering & Science* 52.2 (2012), pp. 438–448. ISSN: 0032-3888. DOI: `10.1002/pen.22102`.

[67] M. Polanco-Loria, A. H. Clausen, T. Berstad, and O. S. Hopperstad. "A constitutive model for thermoplastics intended for structural applications." In: *7th European LS-DYNA conference, Salzburg, Austria*. DYNAmore Germany, pp. 1–3.

[68] D. Porter. *Group Interaction Modelling of Polymer Properties*. CRC Press, 1995. ISBN: 9780824795993.

[69] M. Potenza, P. Coppa, S. Corasaniti, and G. Bovesecchi. "Numerical Simulation of Thermal Diffusivity Measurements With the Laser-Flash Method to Evaluate the Effective Property of Composite Materials." In: *Journal of Heat Transfer* 143.7 (2021). ISSN: 0022-1481. DOI: `10.1115/1.4050995`.

[70] E. L. F. R. Berman and J. M. Ziman. "Thermal conduction in artificial sapphire crystals at low temperatures I. Nearly perfect crystals." In: *Proceedings of the Royal Society of London. Series A. Mathematical and Physical Sciences* 231.1184 (1955), pp. 130–144. ISSN: 0080-4630. DOI: `10.1098/rspa.1955.0161`.

[71] D. Rapp. "Influence of graphite-coating on LFA measurements of thin glass-epoxy composite samples." Montanuniversitaet Leoben, 2020. DOI: `10.13140/RG.2.2.28908.28801`.

[72] S. I. Sandler and L. V. Woodcock. "Historical Observations on Laws of Thermodynamics." In: *Journal of Chemical & Engineering Data* 55.10 (2010), pp. 4485–4490. ISSN: 0021-9568. DOI: `10.1021/je1006828`.

[73] D. V. Schroeder and J. K. Pribram. "An Introduction to Thermal Physics." In: *American Journal of Physics* 67.12 (1999), pp. 1284–1285. ISSN: 0002-9505. DOI: 10.1119/1.19116. URL: https://aapt.scitation.org/doi/pdf/10.1119/1.19116.

[74] K. Shinzato and T. Baba. "A Laser Flash Apparatus for Thermal Diffusivity and Specific Heat Capacity Measurements." In: *Journal of Thermal Analysis and Calorimetry* 64.1 (2001), pp. 413–422. ISSN: 14182874. DOI: 10.1023/A:1011594609521.

[75] N. I. of Standards and Technology, eds. *ITS-90 calibration table.* URL: https://srdata.nist.gov/its90/download/type_k.tab.

[76] Statista. *Revenues from the simulation and analysis market worldwide from 2015 to 2024, by segment (in billion U.S. dollars).* URL: https://www.statista.com/statistics/1192368/worldwide-simulation-and-analysis-market-revenues/.

[77] H. Staudinger. "Über Polymerisation." In: *Berichte der deutschen chemischen Gesellschaft (A and B Series)* 53.6 (1920), pp. 1073–1085. ISSN: 03659488. DOI: 10.1002/cber.19200530627.

[78] W. H. Stockmayer and C. E. Hecht. "Heat Capacity of Chain Polymeric Crystals." In: *The Journal of chemical physics* 21.11 (1953), pp. 1954–1958. ISSN: 0021-9606. DOI: 10.1063/1.1698724.

[79] M.-A. Thermitus and M. Laurent. "New logarithmic technique in the flash method." In: *International Journal of Heat and Mass Transfer* 40.17 (1997), pp. 4183–4190. ISSN: 00179310. DOI: 10.1016/S0017-9310(97)00029-X.

[80] S. Thomke and T. Fujimoto. "The Effect of "Front-Loading" Problem-Solving on Product Development Performance." In: *Journal of Product Innovation Management* 17.2 (2000), pp. 128–142. ISSN: 0737-6782. DOI: 10.1111/1540-5885.1720128.

[81] E. S. Toberer, L. L. Baranowski, and C. Dames. "Advances in Thermal Conductivity." In: *Annual Review of Materials Research* 42.1 (2012), pp. 179–209. ISSN: 1531-7331. DOI: 10.1146/annurev-matsci-070511-155040.

[82] I. A. Tsekmes, R. Kochetov, P. H. F. Morshuis, and J. J. Smit. "Thermal conductivity of polymeric composites: A review." In: *2013 IEEE International Conference on Solid Dielectrics (ICSD)*. IEEE, 62013, pp. 678–681. ISBN: 978-1-4673-4461-6. DOI: 10.1109/ICSD.2013.6619698.

[83] J. Uffink. "COMPENDIUM OF THE FOUNDATIONS OF CLASSICAL STATISTICAL PHYSICS." In: *Philosophy of Physics*. Elsevier, 2007, pp. 923–1074. ISBN: 9780444515605. DOI: 10.1016/B978-044451560-5/50012-9.

[84] *VDI-Wärmeatlas*. Berlin, Heidelberg: Springer Berlin Heidelberg, 2013. ISBN: 978-3-642-19980-6. DOI: 10.1007/978-3-642-19981-3.

[85]   E. S. Watson, M. J. O'Neill, J. Justin, and N. Brenner. "A Differential Scanning Calorimeter for Quantitative Differential Thermal Analysis." In: *Analytical Chemistry* 36.7 (1964), pp. 1233–1238. ISSN: 0003-2700. DOI: `10.1021/ac60213a019`.

[86]   C. R. on the Web. URL: `https://polymerdatabase.com/`.

[87]   A. Wehrl. "General properties of entropy." In: *Reviews of Modern Physics* 50.2 (1978), pp. 221–260. ISSN: 0034-6861. DOI: `10.1103/RevModPhys.50.221`.

[88]   B Wunderlich. "Heat capacity of polymers." In: *Handbook of thermal analysis and calorimetry* 3 (2002), pp. 1–47.

[89]   J. Zhao, J.-W. Jiang, N. Wei, Y. Zhang, and T. Rabczuk. "Thermal conductivity dependence on chain length in amorphous polymers." In: *Journal of Applied Physics* 113.18 (2013), p. 184304. ISSN: 0021-8979. DOI: `10.1063/1.4804237`.

LIST OF FIGURES

LIST OF TABLES